Chapter 4

CORROSION INHIBITION PERFORMANCE OF BENZODIAZEPINES FOR MILD STEEL IN 1M SULPHURIC ACID

4.1 Introduction

Mild steel is widely used in petrochemical, chemical and metallurgical industries. It is also used as construction material owing to its excellent mechanical properties and cost effectiveness. However it easily undergoes corrosion in various environmental conditions especially in acid medium. Acids find various applications in industries as pickling, etching, descaling and cleaning agents but instigate corrosion of mild steel.

The use of inhibitors is the most simple and practical method of protecting metals from corrosion. The corrosion inhibition efficiency is related to their adsorption properties. Adsorption depends on the presence of π-electrons of aromatic systems and heteroatoms which induce greater adsorption of the molecules on the metal surface. Benzodiazepines have these requirements to act as corrosion inhibitors. The first benzodiazepine was accidentally discovered by Leo Sternbach in 1955 and made available in 1960 and marketed as diazepam (valium) since 1963[1]. Benzodiazepines can be easily synthesized by acid catalyzed reaction of *o*-phenylenediamine and ketones or α, β-unsaturated carbonyl compounds. The advantages of the synthesis are the rich source of raw materials, easy synthesis and inexpensive. Benzodiazepines are less toxic, can be naturally degraded into non-toxic substances and are therefore environmentally friendly[2].

1,5-Benzodiazepines have received significant attention because of their accessibility, easy functionalisation and potential pharmacological properties such as anti-inflammatory, anti-anxiety, anti-convulsant and hypnotic activities. 1,5-benzodiazepine represents a privileged scaffold found in compounds active against a variety of target types including peptide hormones, interleukin converting enzymes and inhibitors of mitochondrial adenosine triphosphate hydrolase[3].

The synthetic strategy reported in this thesis involves the reaction of chalkones with *o*-phenylene diamines. Many compounds have been reported in the literature to catalyze the above reactions. Among this sulphated zirconia has attracted much attention

because of its super-acidity, non-toxicity and low cost[4, 5]. It catalyses many reactions under very mild conditions in the vapour phase as well as in the liquid phase. Primarily the chalkones were synthesized by Claisen-Schmidt condensation of acetophenone and substituted aldehydes using alcoholic NaOH.

A Review of literature reveals that though there are large number of reports on the synthesis and pharmacological activities of benzodiazepines, only very few works have been carried out on the use of 1, 5-benzodiazepines as corrosion inhibitors[6-9]. Hence an attempt has been made to synthesize two series of 1, 5-benzodiazepine derivatives and to evaluate their corrosion inhibition properties for mild steel in 1M H_2SO_4.

Molecular structure of the benzodiazepines is given in Table 4.1 and Table 4.2. The synthesized compounds were characterized by FTIR spectra. Figures 4.1- 4.3 show the FTIR spectra of the starting chalkone, benzodiazepines TEBD and MBD respectively. The FTIR spectrum of chalkone shows bands characteristic of -C=O stretching at 1739 cm^{-1} and -HC=CH- at 1624 cm^{-1}. Formation of benzodiazepine has been confirmed by the disappearance of -C=O Stretching band at 1700 cm^{-1} and appearance of a broad strong band at 1595 cm^{-1} for MBD and 1603cm^{-1} for TEBD due to C=N group. A peak around 3100-3200 cm^{-1} characterizes -N-H stretching of benzodiazepine ring. In the case of MBD (Figure 4.3) the -N-H stretching of diazepine ring and –OH stretching of salicylaldehyde moiety merged and appeared as broad band between 3000-3500 cm^{-1}.

NMR Spectra

^{1}H and ^{13}C NMR spectra were reported for representative benzodiazepine- DPBD. The proton NMR spectrum in Figure 4.4 showed the presence of N-H protons as broad band in the range 3.5-4 ppm. –CH$_2$ – protons of the diazepine appear as singlet around 3.2 ppm. The methine proton of the diazepine ring did not appear in the aliphatic region. It has been reported in the literature that the methine proton signal might have mingled with aromatic proton signals due to strong deshielding[10]. Aromatic proton signals appear as multiplets in the region 6.9-8.9 ppm.

The structure of the benzodiazepine was further confirmed by the ^{13}C NMR spectrum which showed (Figure 4.5) three singlets at δ = 29 ppm, 45 ppm and 66 ppm

corresponding to the carbons (a, b, c) of the diazepine ring, while aromatic carbons appear in the region of δ= 119-139 ppm.

4.2 Weight loss method

Weight loss of mild steel specimens were measured after 3 h of immersion in 1M H_2SO_4 containing different concentrations of 1,5-benzodiazepines. The corrosion rate, degree of surface coverage and inhibition efficiency were calculated and recorded in Table 4.3 and 4.4. Corrosion rate of mild steel decreased with increasing concentration of the inhibitors. The degree of surface coverage θ increased as the concentration of the inhibitors increased. This shows that the compounds inhibit corrosion by adsorption on the steel surface. As concentration of the inhibitors increases more molecules get adsorbed and block the active sites for corrosion. All the compounds showed significant inhibition effect on mild steel and the efficiency reached up to 97% depending on the substituent groups attached. In series I, the compound having two phenyl substituents and a methyl group (MDPBD) shows 83% efficiency. Benzodiazepines with methyl/ethyl group substituted on the diazepine ring showed 65% and 68% efficiency respectively. Benzodiazepines having substituents in the phenyl ring showed >80% efficiency with TMPBD (trimethoxy phenyl substituted) displaying 97% efficiency.

4.3 Effect of temperature

The effect of increasing the temperature on the corrosion rate of mild steel in 1M H_2SO_4 containing 200 ppm of the benzodiazepines was studied in the temperature range from 303K-333K by weight loss measurements. As the temperature increases, the corrosion rate increases and hence the inhibition efficiencies of the two series of benzodiazepines decrease (Table 4.5 and 4.6). Analysis of the data shows that, as the temperature is increased from 303K to 313K, the efficiency of the compounds decreased by 10-14%. After that, the decrease in efficiency was less and about 5-9% decrease was noted. The trimethoxy phenyl benzodiazepine showed 71% efficiency even at 333K proving its efficiency in the temperature range studied.

The activation energy E_a represents the energy necessary for a molecule to possess, in order to react; in this case for corrosion process, is calculated using the Arrhenius equation

$$\text{Corrosion rate} = A \exp\left(\frac{-E_a}{RT}\right)$$

Taking log,

$$\text{Log corrosion rate} = \log A - E_a/RT$$

Where A= Arrhenius pre exponential factor, E_a = Activation energy for the corrosion process. A plot of log corrosion rate vs. 1/T was found to be linear (Figure 4.6). E_a was obtained from the slopes of the lines (E_a= slope * 2.303).

The enthalpy of activation, ΔH^* is obtained from the equation,

$$\Delta H^* = E_a - RT$$

The change in free energy of activation ΔG^* is defined as the difference in the activation energies between the activated state and initial state of the reacting species[11] and is calculated using Eyrings equation,

$$r = \frac{kT}{h} \cdot e^{\frac{-\Delta G^*}{RT}}$$

Where r is the rate constant for corrosion process and is equated to corrosion rate. k= Boltzmann's constant, h= Planck's constant and T is the absolute temperature. The change in entropy of activation at any temperature is given by

$$\Delta G^* = \Delta H^* - T\Delta S^*$$

The value of E_a, ΔH^*, ΔG^* and ΔS^* obtained are recorded in Table 4.7 and 4.8. A comparison of the thermodynamic parameters for mild steel immersed in 1M H_2SO_4 (blank) and 1M H_2SO_4 containing the benzodiazepines showed that E_a is higher for inhibited system (79.63 kJ/mol for DPBD and 89.73 kJ/mol for TMPBD) against blank acid value of 27.7 kJ/ mol. This shows that the presence of inhibitors increases the activation energy for corrosion and hence decreases the corrosion rate. The ΔH^* values are positive and increased in the presence of benzodiazepines by about 32-62 kJ/mol. This reveals that the dissolution of steel is endothermic. Usually enthalpy is more for slower reactions which means that the inhibitor's presence slowed down the corrosion process. ΔG^* values are negative and are in the range of -20 kJ/mol indicating that the physisorption of the inhibitor's occur spontaneously. Change in entropy ΔS^* of the

uninhibited and inhibited systems is positive, but the values are more for inhibited mild steel compared to uninhibited mild steel ($\Delta S^* = 0.15$ kJ mol^{-1}K^{-1}) which may be attributed to an increase in disorder due to adsorption of the compounds on steel surface. Analysis of the table show that the values are all high in presence of 2, 4-diphenylbenzodiazepine (series I) and trimethoxyphenylbenzodiazepine (series II) showing their excellent performance compared to other compounds studied.

4.4 Adsorption isotherm

In aqueous phase the action of inhibitor on the metallic corrosion inhibition is assumed to be due to adsorption at the metal-solution interface by replacement of adsorbed water molecules. The interaction between the inhibitor and mild steel surface can be understood from the adsorption isotherms. All the isotherms are represented by the general form

$$f(\theta, x) \exp(-\alpha\,\theta) = k\,C$$

Where α is the molecular interaction parameter which depends on the molecular interactions in the adsorbed layer and on the degree of heterogeneity of the surface, $f(\theta, x)$, the configurational factor, which depends upon the physical model and assumptions behind the derivation of the isotherm, C is the inhibitor concentration, θ is the surface coverage, x is the size ratio and k is the equilibrium constant of adsorption process[12].

The degree of surface coverage obtained from mass loss measurements at different concentrations of the benzodiazepines were fitted graphically to various adsorption isotherms viz.., Langmuir, Temkin, Flory Huggins and El-Awady model. Correlation coefficient R^2 was used to determine the best fit. Langmuir isotherm is the basic one and is given as,

$$\theta = \frac{K_{ads}\,C_{inh}}{1 + K_{ads}\,C_{inh}}$$

Where K_{ads} is the equilibrium constant for the adsorption-desorption process[13]. This equation is rearranged to

$$\frac{C_{inh}}{\theta} = \frac{1}{K_{ads}} + C_{inh}$$

C_{inh} is the concentration of the inhibitor; θ is the fractional surface coverage. Plots of C_{inh} / θ vs. C_{inh} were found to be linear (Figure 4.7) with R^2 values of 0.98 to 0.99

suggesting that the adsorption of the benzodiazepines on mild steel obeyed Langmuir isotherm. The K_{ads} is obtained from the intercepts of the lines on the Y axis.

K_{ads} and free energy change of adsorption are related as,

$$\Delta G^{\circ}_{ads} = -RT \ln(55.5\, K_{ads})$$

Where 55.5 is the molar concentration of water, R is the universal gas constant and T is the temperature in Kelvin. The calculated ΔG°_{ads} values are tabulated (Table 4.9 and 4.10). The values are all negative and the absolute values approach than 40 kJ/mol. This indicates spontaneous adsorption of the benzodiazepines through electrostatic attraction between the metal ions on the surface and the inhibitor species. Afterwards there may be formation of chemical bonds via electron transfer reaction. The values of equilibrium constants are in the range 1.1×10^4 to 3.3×10^4 which is high suggesting strong adsorption.

4.5 Electrochemical impedance spectroscopy (EIS)

Impedance method provides information about the kinetics of the electrode processes and the surface properties of the investigated systems. The technique is based on the measurement of the impedance of the double layer at the metal/solution interface. The real part Z′ and imaginary part Z″ of the cell impedance were measured in ohm cm^2 at various frequencies and plotted in the form of Nyquist plots. Figures 4.8 - 4.17 represents the Nyquist plots of mild steel specimens in 1M H_2SO_4 without and with various concentrations of the benzodiazepines. These plots are semicircles which intersect the real axis at higher and lower frequencies. At high frequency end the intercept corresponds to the solution resistance R_s and at lower frequency end corresponds to the sum of R_s and the charge transfer resistance R_t. The difference between the two values gives R_t. The value of R_t is a measure of electron transfer across the exposed areas of the metal surface and inversely proportional to the rate of corrosion. It is evident from the plots that the impedance of the inhibited mild steel increases with increase in inhibitor concentration. Consequently the inhibition efficiency increased. The benzodiazepines get adsorbed on the mild steel/acid solution interface and produce a barrier for the metal to diffuse in to solution and the barrier increases with increasing concentration.

Impedance behavior can be explained by equivalent circuit models that enable to calculate the numerical values of double layer capacitance and charge transfer resistance corresponding to the physical and chemical properties of the electrochemical system under investigation. The simple equivalent circuit that fits many electrochemical systems composed of solution resistance R_s, in series with a parallel combination of charge transfer resistance R_t and double layer capacitance C_{dl}.
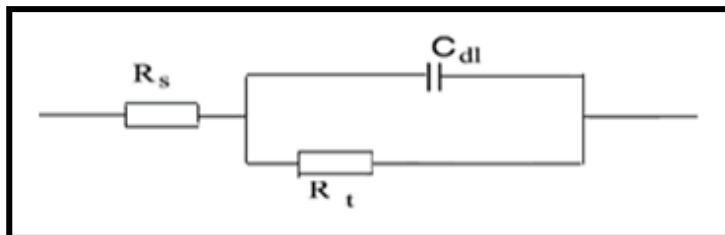
Equivalent circuit model

The charge transfer resistance values R_t are calculated from the difference in impedance at lower and higher frequencies. The double layer capacitance C_{dl} is used to characterize the double layer which is believed to be formed at the metal-solution interface of systems having non-ideal capacitive behaviors i.e., corroding metal in aqueous solution[14].

The values of R_t and C_{dl} obtained for mild steel in 1M H_2SO_4 (blank and inhibited) are given in Table 4.11 and 4.12.

The percentage inhibition efficiency is calculated from R_t values as,

$$IE\ (\%) = \frac{R_{t(inh)} - R_{t(blank)}}{R_{t(inh)}} \times 100$$

Where $R_{t\ (inh)}$ and $R_{t\ (blank)}$ are the charge transfer resistances for mild steel immersed in 1M H_2SO_4 with inhibitor and without inhibitors respectively. It is clear that addition of benzodiazepines into the sulphuric acid solution caused an increase in the charge transfer resistance R_t and a decrease in C_{dl} values. R_t is increased to a maximum value of 160 ohm.cm^2 for TEBD (series I) and TMPBD (series II) which show the maximum inhibition efficiency of 88% at 200 ppm concentration.

The double layer capacitance is related to the thickness of the double layer[15] as,

$$C_{dl} = \frac{\epsilon \, \epsilon_o A}{d}$$

Where ϵ_o is the vacuum dielectric constant, ϵ is the dielectric constant of the medium, d is the thickness of the electrical double layer and A is the surface area of the electrode. The decrease in double layer in the presence of benzodiazepines from the blank acid value of 46.7µF/cm^2 is therefore attributed to the replacement of adsorbed water molecules (high dielectric constant) by the organic compounds (low dielectric constant) on the mild steel surface and also due to increased thickness of the double layer, with increased concentration of the benzodiazepines.

4.6 Potentiodynamic polarization measurements

Figure 4.18 - 4.27 show the anodic and cathodic polarization curves of mild steel in 1M sulphuric acid solution without and with benzodiazepine derivatives at 303 ± 1K. It is evident that, addition of benzodiazepine decreases the current density in the cathodic region of polarization, they decrease the current density in the anodic domain at the higher concentration tested (200 ppm). There is no considerable shift of the polarization curves in either direction suggesting that the studied benzodiazepine derivatives are of mixed type.

The electrochemical parameters derived from the Tafel polarization curves such as corrosion current density I_{corr}, corrosion potential E_{corr}, anodic and cathodic Tafel constants b_a and b_c (obtained by extrapolation of the linear parts of Tafel lines to E_{corr} are recorded in Table 4.13 and 4.14. Inhibition efficiency was calculated using the equation,

$$IE \, (\%) = \left(1 - \frac{I_{corr}}{I^o_{corr}}\right) X \, 100$$

Where, I_{corr} and I^o_{corr} are the corrosion current densities in the absence and presence of benzodiazepine derivatives. In the first series of compounds, maximum reduction in corrosion current was observed for mild steel immersed in 1M H_2SO_4 containing 2-methyl- 2,4-diphenyl benzodiazepine (MDPBD) (93 µ A/cm^2) compared to that in blank acid 414 µ A/cm^2 and the IE(%) calculated was 77.43%. Among the phenyl substituted benzodiazepines, trimethoxy phenyl benzodiazepine (TMPBD) remarkably

decreased the corrosion current density of mild steel to 35 μ A/cm^2 with a percent inhibition efficiency of 91.54. The significant reduction in corrosion current density indicated the effective corrosion protection performance of these compounds. The E_{corr} values are shifted slightly towards less negative direction by about 20-35 mV. It has been reported that, if the displacement in E_{corr} is more than ± 85 mV vs. saturated calomel electrode compared to the corrosion potential of the blank, the inhibitor acts as pure cathodic or anodic type[16]. If the change is less than 85 mV vs. SCE, the inhibitor is classified as mixed type. Maximum shift of E_{corr} in the present study was found to be 30 mV for EPBD indicating that the benzodiazepines are mixed type. The anodic and cathodic slopes b_a and b_c are both affected confirming that the tested compounds are mixed type inhibitors.

4.7 Surface morphology analysis

SEM and AFM studies were carried out to analyze the surface morphology of the mild steel samples immersed in 1M H_2SO_4 without and with a representative benzodiazepine DPBD. The SEM photomicrographs of the polished mild steel surface exposed to uninhibited and inhibited 1M H_2SO_4 solution are shown in Figure 4.28a - 4.28c. The polished mild steel sample in Figure 4.28a shows smooth surface without any defects such as cracks and pits. The surface of the mild steel immersed in 1M H_2SO_4, suffered from severe corrosion as evidenced by the SEM micrograph (Figure 4.28b) which shows damaged heterogeneous morphology. The damage is considerably decreased in the presence of the benzodiazepine derivative (DPBD) as seen from Figure 4.28c which shows the presence of particles of the compounds. The decrease in corrosive damage may be due to the deposition of adsorbed benzodiazepine molecules on mild steel surface which protected the surface from the aggressive medium.

The EDX spectra were used to determine the elements present on the mild steel surface after 3 h of exposure to 1M H_2SO_4 with and without 200 ppm of benzodiazepine. The EDX spectrum (Figure 4.29a) of steel sample shows Fe, C, S and O signals when immersed in 1M H_2SO_4 which are due to the formation of passive film containing oxides and sulphides. In the presence of the inhibitors (Figure 4.29b) additional lines for C and N are obtained demonstrating the presence of adsorbed benzodiazepines on the mild steel surface. The data are presented in Table 4.15.

SEM results are supported by AFM studies. The AFM images were recorded for polished mild steel surface and surface exposed to uninhibited and inhibited acid solution with 200 ppm DPBD at room temperature in the range 0-10 μm. The three dimensional AFM morphologies are depicted in Figure 4.30a – 4.30c. The average roughness S_a (the average deviation of all points roughness profile from a mean line over the evaluation length), root mean square roughness S_q (the average of the measured height deviations taken within the evaluation length and measured from the mean line) and the maximum peak to valley (P-V) height (largest single peak-to-valley height in five adjoining sampling heights) were obtained from the AFM micrographs[8] and are summarized in Table 4.16.

The values of S_q, S_a and P-V height for the polished mild steel are 137.43 nm, 104.92 nm, 1005.46 nm respectively which shows a smooth homogeneous surface. The values for uninhibited and inhibited steel surface show that unprotected steel surface immersed in 1M H_2SO_4 has greater roughness due to corrosion. The roughness is significantly reduced from S_q 202.54 nm to 142.84 nm, S_a 160.65 to 107.57 nm in the presence of benzodiazepine which therefore inhibited the corrosion of steel by formation of a protective film. The roughness values obtained for mild steel in the presence of benzodiazepines is only slightly higher compared to polished mild steel.

4.8 FTIR spectra

The FTIR spectroscopy is also used to ascertain the formation of adsorbed layer of the benzodiazepine on the steel surface. Figure 4.31 and 4.32 show the FTIR spectra recorded for mild steel surface after immersion in 1M H_2SO_4 without and with DPBD as inhibitor. No characteristic bands were observed for mild steel immersed in 1M H_2SO_4, except in the range 550 cm^{-1} due to Fe-O linkage of the passive layer of iron oxide. The specimen immersed in 1M H_2SO_4 containing DPBD show low intensity bands at 3500 cm^{-1}, 1534 cm^{-1} and 650 cm^{-1} characteristics of –N-H-, -C=N and Fe-N bonds confirming the presence of adsorbed inhibitors.

4.9 Chemical structure of the inhibitors and corrosion inhibition performance

Heterocyclic compounds are effective corrosion inhibitors. The primary factor in the process of inhibition is adsorption of the molecules on the metal surface. The extent of adsorption depends on several physicochemical properties of the inhibitor molecule

like functional group, geometry, electron density at the heteroatoms, π-electrons and planarity of the molecule.

A heterocyclic organic molecule comprehensively acts in reducing the corrosion rate. In acid media, electron rich centers in the molecule get protonated to become cations and electrostatically bind to the cathodic sites of metal and reduce cathodic corrosion reaction. Electron rich centers of unprotonated molecules bind to the anodic sites on metal surface and hinder anodic reaction[17].

In the present study two series of benzodiazepines have been synthesized and their corrosion inhibition performance for mild steel in 1M H_2SO_4 has been investigated. Series-I compounds differ in substituents on the seven membered ring. Methyl, ethyl and phenyl groups were substituted. The order of efficiency based on all the three methods is,

MDPBD > DPBD > MPBD > TEBD ~ TMBD

$(2, 4\text{-}(Ph)_2\text{-}2\text{-}Me) > 2, 4\text{-}(Ph)_2 > 2\text{-}Ph\text{-}4\text{-}Me > 2, 2, 4\text{-}(Et)_3 \sim 2, 2, 4\text{-}(Me)_3$
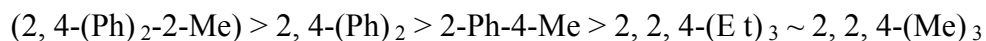
It is well known that electron donating alkyl groups increase the electron density on the main adsorption centre and hence enhance the inhibition efficiency. In the current study, phenyl substituted benzodiazepines showed higher inhibition than alkyl substituted derivatives. A perusal of literature[17, 18] revealed that an aromatic substituent group remarkably increases the inhibition efficiency of a compound. While investigating the bisthiadiazoles, Quraishi and Singh[19] have reported that presence of a benzene ring between the thiadiazole rings makes the molecule planar in addition to providing additional π-electrons and hence the molecule gets firmly adsorbed on the metal surface. A similar explanation can be given for the better performance of MDPBD which has two phenyl rings and an electron donating methyl group. DPBD comes next in the order which has two phenyl rings, MPBD has one phenyl ring and a methyl group shows slightly lower inhibition efficiency. The triethyl and trimethyl derivatives show least efficiency (60-70%), in spite of the presence of electron donating alkyl groups.

In series-II, substituents are introduced on one of the phenyl ring. The order of inhibition being,

TMPBD > EPBD > MEPBD > PBD > MBD

An organic corrosion inhibitor has an anchoring group which binds on to the metal. The back bone bears anchoring group and substituents groups and provides surface coverage. The substituent groups supplement electronic strength and surface coverage. Introduction of substituents in different position of the rings affects the availability of electron pairs in the molecule for binding with the metal surface. Most p-substituents undergo resonance with the reaction centre. Based on Hammet σ values, the electron charge density at the reaction centre would decrease in the order OH > -OCH$_3$ > -CH$_3$ > H > Cl. If polar effects are only operating, inhibition efficiency of the compounds having the above substituents follows the same order. But Hammet pointed out that substantial resonance contribution to the net electron releasing effect exists for p-OCH$_3$ group (σ = -0.27). p- OH group has been reported to form soluble complex and hence the compounds are less efficient[20]. The superior performance of TMPBD has been attributed to the presence of 3 –OCH$_3$ groups in the meta and para position in line with the electron releasing nature through resonance. EPBD and MEPBD have –OH group in para and –OEt / OCH$_3$ in the m-position. The lower inhibition efficiency may be due to the solubility of the adsorbed inhibitor in the corrosion medium.

References

1. Shorter E, *A Historical Dictionary of Psychiatry*, Oxford University Press, (2005) 41.

2. Yan X, Shang M S, Yuanwei L, Binzhou University *Patent CN 104232073A* (2014).

3. Sagar A D, Tigote R M, Haval K P, Sarnikar Y P, Sunil Khapate, *International Journal of Scientific and Research Publications*, **3** (2013) 602.

4. Hua W, Sommer J, *Appl Catal A Gen*, **227** (2002) 279.

5. Reddy B M, Sreekanth P M, *Tetrahedron Lett.*, **44** (2003) 4447.

6. Niouri W, Zerga B, Sfaira M, Taleb M, Hammouti B, Ebn Touhami M, Al-Deyab S S, Benzeid H, Essassi E M, *Int. J. Electrochem.Sci*, **7** (2012) 10190.

7. Niouri W, Zerga B, Sfaira M, Taleb M, Ebn Touhami M, Hammouti B, Mcharfi M, Al-Deyab S S, Benzeid H, Essassi E M, *Int. J. Electrochem. Sci*, **9** (2014) 8283.

8. Sikine M, Kandri Rodi Y, Elmsellem H, Krim O, Ouzidan Y, Kandri Rodi A, Ouazzani Chahdi F, Sebbar N K, Essassi E M, *J. Mater. Environ. Sci.,* **7** (2016) 1386.

9. Laabaissi T, Bouassiria M, Oudda H, Zarrok H, Zarrouk A, Elmidaoui A, Lakhirissi L, Lakhrissi B, Essassi E M, Touir R, *J. Mater. Environ. Sci.*, **7** (2016)1538.

10. Ilango S S, Remya P U, Ponnusamy S, *Ind. J. Chem.*, 52(B) (2013) 136.

11. Elmorsi M A, Hassanein A M, *Corros. Sci.,* **41** (1999) 2337.

12. El-Awady A A, Abd-El-Nabey B A, Aziz S G, *J. Electrochem. Soc.* **139** (1992) 2149.

13. Singh A, Ebenso E E, Quraishi M A, Lin Y, *Int. J. Electrochem. Sci.* **9** (2014) 7495.

14. Ashassi Sorkhabi H, Shaabani B, Seifzadeh D, *Appl. Surf. Sci.,* **239** (2008) 154.

15. Ahamad I, Prasad R, Ebenso E E, Quraishi M A, *Int. J. Electrochem. Sci*, **7** (2012) 3436.

16. Nataraja S E, Venkatesha T V, Praveen B M, *Der Pharma Chem.*, **3** (2011) 388.

17. Badr G E, *Corros. Sci.*, **51** (2009) 2529.

18. Benabdellah M, Touzani R, Aouniti A, Dafali A, El Kadiri S, Hammouti B, Benkaddour M, *Mater. Chem. Phys.*, **105** (2007) 373.

19. Singh A K, Quraishi M A, *Corros. Sci.,* **52** (2010) 1373.

20. Fouda A S, Mostafa H A, Moussa M N, *Port. Electrochim. Acta.*, **22** (2005) 275.
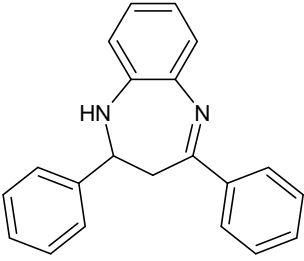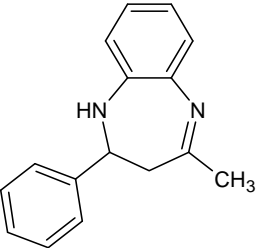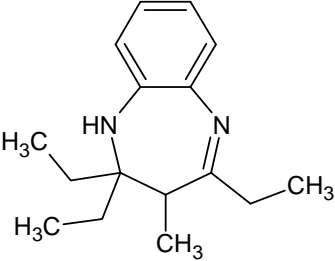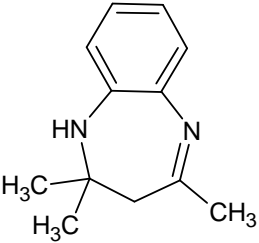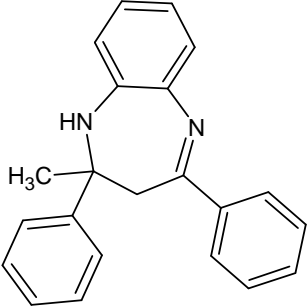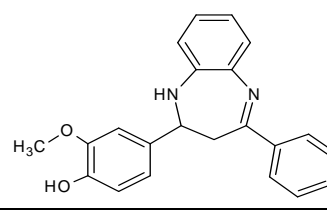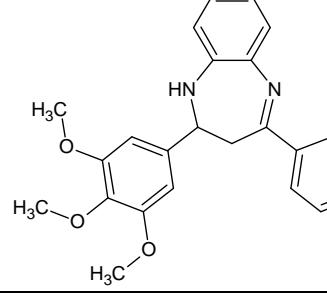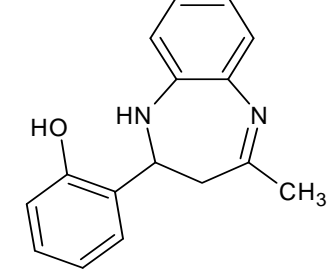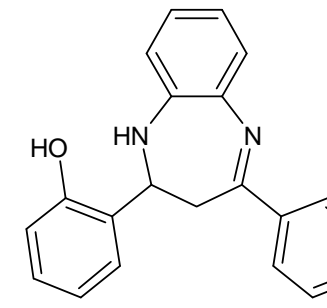
Tables
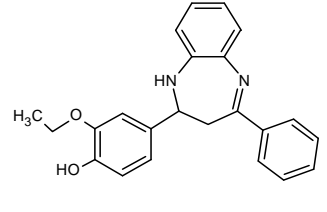
Table 4.1 Molecular Structure of Benzodiazepines

Benzodiazepines with substituent on the diazepine ring –**Series I**

Structure	IUPAC Nomenclature	Abbreviation	Melting point ($^{\circ}$C)
	2,4-diphenyl-2,3-dihydro-1*H*-1,5-benzodiazepine	DPBD	136-137
	2-phenyl-4-methyl-2,3-dihydro-1*H*-1,5-benzodiazepine	MPBD	120-123
	2,2,4-triethyl-3-methyl-2,3-dihydro-1*H*-1,5-benzodiazepine	TEBD	143-144
	2,2,4-trimethyl-2,3-dihydro-1*H*-1,5-benzodiazepine	TMBD	126
	2-methyl-2,4-diphenyl-2,3-dihydro-1*H*-1,5-benzodiazepine	MDPBD	151-152

Table 4.2 Benzodiazepines with Substituent on phenyl ring-**Series II**

Structure	IUPAC Nomenclature	Abbreviation	Melting Point (°C)
	2-(3-ethoxy-4-hydroxyphenyl)- 2-phenyl 2,3-dihydro-1*H*-1,5-benzodiazepine	EPBD	122-124
	2-(3-methoxy-4-hydroxyphenyl)- 2-phenyl 2,3 –dihydro-1*H*-1,5-benzodiazepine	MEPBD	114
	2-(3,4,5-trimethoxyphenyl)- 4-phenyl -2,3-dihydro-1*H*-1,5-benzodiazepine	TMPBD	63-64
	2-(2-hydroxyphenyl)-4-methyl-2,3-dihydro-1*H*-1,5-benzodiazepine	MBD	110
	2-(2-hydroxyphenyl)-4-phenyl-2,3-dihydro-1*H*-1,5-benzodiazepine	PBD	128-129

Table 4.3 Inhibition efficiencies of various concentrations of benzodiazepines (series I) for corrosion of mild steel in 1M H_2SO_4 obtained by weight loss measurements at 303 ± 1 K

Name of the inhibitor	Concentration (ppm)	Weight loss (g)	Inhibition efficiency (%)	Degree of Surface coverage (θ)	Corrosion rate (mpy)
BLANK		0.2656			17466.71
MDPBD	10	0.1097	58.69	0.5869	7214.22
	50	0.09	66.11	0.6611	5918.69
	100	0.0755	71.57	0.7157	4965.12
	150	0.0622	76.58	0.7658	4090.47
	200	0.0483	83.05	0.8305	2959.34
DPBD	10	0.1185	55.38	0.5538	7792.94
	50	0.0986	62.87	0.6287	6484.25
	100	0.0865	67.43	0.6743	5688.51
	150	0.0765	71.19	0.7119	5030.88
	200	0.06	77.40	0.7740	3945.79
MPBD	10	0.1438	45.85	0.4585	9456.75
	50	0.1225	53.87	0.5387	8055.99
	100	0.1126	57.60	0.5760	7404.93
	150	0.0909	65.77	0.6577	5977.87
	200	0.069	74.02	0.7402	4537.66
TEBD	10	0.1488	43.97	0.4397	9785.56
	50	0.1256	52.71	0.5271	8259.86
	100	0.1146	56.85	0.5685	7536.46
	150	0.1002	62.27	0.6227	6589.47
	200	0.0848	68.07	0.6807	5563.56
TMBD	10	0.1532	42.31	0.4231	10074.9
	50	0.1414	46.76	0.4676	9298.92
	100	0.1198	54.89	0.5489	7878.43
	150	0.1022	61.52	0.6152	6721.00
	200	0.092	65.36	0.6536	6037.06

Table 4.4 Inhibition efficiencies of various concentrations of benzodiazepines (series II) for corrosion of mild steel in 1M H_2SO_4 obtained by weight loss measurements at 303 ± 1 K

Name of the inhibitor	Concentration (ppm)	Weight loss (g)	Inhibition efficiency (%)	Degree of Surface coverage (θ)	Corrosion rate (mpy)
BLANK	-	0.2656	-	-	17466.71
TMPBD	10	0.0688	74.09	0.7409	4524.51
	50	0.0605	77.22	0.7722	3978.67
	100	0.0415	84.37	0.8437	2729.17
	150	0.0258	90.28	0.9028	1696.69
	200	0.0063	97.62	0.9762	414.30
EPBD	10	0.0769	71.04	0.7104	5057.19
	50	0.0628	76.35	0.7635	4129.93
	100	0.0435	83.62	0.8362	2860.7
	150	0.0346	86.97	0.8697	2275.40
	200	0.0135	94.91	0.9491	887.80
MEPBD	10	0.0888	66.56	0.6656	9121.35
	50	0.0779	70.67	0.7067	5122.95
	100	0.0585	77.97	0.7797	4715.22
	150	0.0425	83.99	0.8399	900.95
	200	0.0246	90.73	0.9073	526.10
PBD	10	0.0875	67.05	0.6705	5754.28
	50	0.0735	72.32	0.7232	4833.59
	100	0.0615	76.84	0.7684	4044.43
	150	0.0473	82.19	0.8219	3110.6
	200	0.0366	86.21	0.8621	2406.93
MBD	10	0.0928	65.06	0.6506	6102.82
	50	0.0775	70.82	0.7082	5096.65
	100	0.0665	74.96	0.7496	4373.19
	150	0.0566	78.68	0.7868	3722.19
	200	0.0513	80.68	0.8068	3373.65

Table 4.5 Corrosion parameters for mild steel in 1M H_2SO_4 in the absence and presence of 200 ppm of benzodiazepines (series I) from weight loss measurements at different temperatures.

Name of the inhibitor	Temperature (K)	Weight loss (g)	Inhibition efficiency (%)	Degree of Surface coverage (θ)	Corrosion rate (mpy)
BLANK	303	0.0885	-	-	17466.71
	313	0.1152	-	-	22727.6
	323	0.1443	-	-	28468.69
	333	0.2486	-	-	49045.85
MDPBD	303	0.015	83.05	0.8305	2959.32
	313	0.034	70.48	0.7048	6707.79
	323	0.054	62.57	0.6257	10653.56
	333	0.1075	56.75	0.5675	21208.48
DPBD	303	0.02	77.40	0.7740	3945.76
	313	0.0413	64.14	0.6414	8148.00
	323	0.0645	55.30	0.5530	12725.09
	333	0.1286	48.27	0.4827	25371.26
MPBD	303	0.023	74.01	0.7401	4537.62
	313	0.0405	64.84	0.6484	7990.17
	323	0.0695	51.83	0.5183	13711.53
	333	0.1336	46.25	0.4625	26357.7
TEBD	303	0.0282	68.13	0.6813	5563.52
	313	0.0516	55.20	0.5520	10180.07
	323	0.0779	46.01	0.4601	15368.75
	333	0.14922	39.97	0.3997	29439.35
TMBD	303	0.0306	65.42	0.6542	6037.01
	313	0.0546	52.60	0.5260	10771.94
	323	0.0846	41.37	0.4137	16690.58
	333	0.1683	32.30	0.3230	33203.61

Table 4.6 Corrosion parameters for mild steel in 1M H_2SO_4 in the absence and presence of 200 ppm of benzodiazepines (series II) from weight loss measurements at different temperatures.

Name of the inhibitor	Temperature(K)	Weight loss (g)	Inhibition efficiency (%)	Degree of Surface coverage (θ)	Corrosion rate (mpy)
TMPBD	303	0.0021	97.62	0.9762	414.30
	313	0.0178	84.54	0.8454	3511.73
	323	0.0315	78.17	0.7817	6214.57
	333	0.0708	71.52	0.7152	13968.01
EPBD	303	0.0045	94.91	0.9491	887.79
	313	0.0213	81.51	0.7609	4202.23
	323	0.0345	76.09	0.7609	6806.44
	333	0.0788	68.30	0.6830	15546.31
MEPBD	303	0.0082	90.73	0.9073	1617.76
	313	0.0238	79.34	0.7934	4695.45
	323	0.0388	73.11	0.7311	7654.78
	333	0.0852	65.72	0.6572	16808.96
PBD	303	0.0122	86.21	0.8621	2406.91
	313	0.032	72.22	0.7222	6313.22
	323	0.0504	65.07	0.6507	9943.32
	333	0.1040	58.16	0.5816	20517.97
MBD	303	0.0171	80.67	0.8067	3373.62
	313	0.034	70.48	0.7048	6707.79
	323	0.056	61.19	0.6119	11048.14
	333	0.1084	56.39	0.5639	21386.04

Table 4.7 Thermodynamic parameters for the corrosion of mild steel in 1M H_2SO_4 without and with 200 ppm of the benzodiazepines (series I)

Name of the inhibitor	E_a (kJ/mol)	ΔG^* (kJ/mol)	ΔH^*(kJ/mol)	ΔS^* (kJ mol^{-1} K^{-1})
BLANK	27.7	-21.56	25.18	0.15
MDPBD	60.32	-23.50	57.80	0.26
DPBD	79.73	-23.18	77.21	0.33
MPBD	71.68	-23.03	69.76	0.30
TEBD	45.34	-22.80	42.82	0.21
TMBD	72.02	-22.72	69.72	0.30

Table 4.8 Thermodynamic parameters for the corrosion of mild steel in 1M H_2SO_4 without and with 200 ppm concentration of the benzodiazepines (series II)

Name of the inhibitor	E_a (kJ/mol)	ΔG^* (kJ/mol)	ΔH^* (kJ/mol)	ΔS^* (kJ mol^{-1} K^{-1})
BLANK	27.7	-21.56	25.18	0.15
TMPBD	89.73	-25.65	87.21	0.37
EPBD	79.82	-24.81	77.30	0.33
MEPBD	64.94	-25.39	62.42	0.28
PBD	78.09	-23.72	75.57	0.32
MBD	59.65	-23.35	57.13	0.26

Table 4.9 Langmuir adsorption isotherm parameters for benzodiazepines (series I) at 303 ± 1 K

Compound	K_{ads} (M^{-1}) X 10^4	R^2	$-\Delta G^{\circ}_{ads}$ (kJ/mol)
MDPBD	2.5	0.9941	35.63
DPBD	2.5	0.993	35.63
MPBD	1.42	0.9930	34.20
TEBD	1.25	0.9893	33.88
TMBD	1.11	0.9945	33.58

Table 4.10 Langmuir adsorption isotherm parameters for benzodiazepines (series II) at 303 ± 1 K

Compound	K_{ads} (M^{-1}) X 10^4	R^2	$-\Delta G^{\circ}_{ads}$ (kJ/mol)
TMPBD	3.3	0.9921	36.33
EPBD	3.3	0.9930	36.33
MEPBD	2.5	0.9915	35.63
PBD	3.3	0.9913	36.33
MBD	1.42	0.9993	34.20

Table 4.11 Impedance parameters for the corrosion of mild steel in 1M H_2SO_4 for selected concentrations of benzodiazepines (series I) at 303 ± 1 K.

Name of the inhibitor	Concentration (ppm)	R_t (ohm.cm^2)	C_{dl} (μ F/cm^2)	Inhibition efficiency (%)
BLANK	-	18.00	46.7	-
MDPBD	10	62.00	32.2	70.96
	100	78.00	25.9	76.92
	200	82.00	17.7	78.04
DPBD	10	50.00	31.0	64.00
	100	78.00	29.7	76.92
	200	90.00	29.5	80.00
MPBD	10	49.00	32.7	63.26
	100	58.00	31.1	68.96
	200	78.00	30.8	76.92
TEBD	10	40.00	33.9	55.00
	100	70.00	27.8	74.28
	200	160.00	25.4	88.75
TMBD	10	35.00	31.1	48.57
	100	45.00	30.8	60.00
	200	60.00	24.9	70.00

Table 4.12 Impedance parameters for the corrosion of mild steel in 1M H_2SO_4 for selected concentrations of benzodiazepines (series II) at 303 ± 1 K.

Name of the inhibitor	Concentration (ppm)	R_t (ohm.cm^2)	C_{dl} (μ F/cm^2)	Inhibition efficiency (%)
BLANK	-	18.00	46.7	-
TMPBD	10	65.00	31.4	72.30
	100	105.00	26.1	82.85
	200	160.00	24.9	88.75
EPBD	10	60.00	30.8	70.00
	100	78.00	24.4	76.92
	200	120.00	19.7	85.00
MEPBD	10	55.00	32.2	67.27
	100	69.00	25.9	73.91
	200	105.00	17.7	82.85
MBD	10	52.00	29.5	65.38
	100	65.00	22.7	72.30
	200	115.00	19.7	84.34
PBD	10	50.00	29.5	64.00
	100	65.00	25.2	72.30
	200	113.00	20.1	84.07

Table 4.13 Corrosion parameters for corrosion of mild steel in 1M H_2SO_4 with selected concentrations of benzodiazepines (series I) by potentiodynamic polarization method at 303 ± 1 K.

Name of the inhibitor	Concentration (ppm)	Tafel slopes (mV/dec)		E_{corr} mV)	$I_{corr}(\mu$ A/cm^2)	Inhibition efficiency (%)
		b_a	$-b_c$			
BLANK	-	68	167	-480.0	414.0	-
DPBD	10	60	173	-470.0	240.0	42.02
	100	58	164	-482.3	156.0	62.31
	200	52	167	-500.0	120.0	71.01
MPBD	10	64	152	-490.0	252.0	39.13
	100	53	153	-470.0	180.0	56.52
	200	42	156	-460.2	135.00	67.39
TEBD	10	61	164	-475.4	260.30	37.12
	100	62	159	-470.5	210.4	49.17
	200	62	157	-460.0	160.00	61.35
TMBD	10	62	148	-490.0	280.00	32.36
	100	58	158	-485.0	240.60	41.88
	200	48	171	-460.0	170.00	58.93
MDPBD	10	61	154	-476.3	182.0	56.03
	100	51	140	-472.8	130.2	68.55
	200	57	155	-470.4	93.4	77.43

Table 4.14 Corrosion parameters for corrosion of mild steel in 1M H_2SO_4 with selected concentrations of benzodiazepines (series II) by potentiodynamic polarization method at 303 ± 1 K.

Name of the inhibitor	Concentration (ppm)	Tafel slopes (mV/dec)		E_{corr} (mV)	$I_{corr}(\mu A/cm^2)$	Inhibition efficiency (%)
		b_a	$-b_c$			
BLANK	-	68	167	-480.0	414.0	-
TMPBD	10	64	160	-490.0	73.0	82.36
	100	61	165	-460.0	54.0	86.95
	200	59	178	-458.0	35.00	91.54
EPBD	10	62	159	-475.0	120.00	71.01
	100	56	157	-471.1	93.00	77.52
	200	58	163	-450.4	53.00	87.19
MEPBD	10	54	152	-478.0	150.0	63.76
	100	56	167	-470.0	130.00	68.59
	200	43	134	-460.0	66.5	83.93
PBD	10	60	155	-485.0	225.0	45.65
	100	50	143	-482.0	150.0	63.76
	200	46	174	-470.0	80.00	80.67
MBD	10	64	155	-482.0	250.0	39.61
	100	57	135	-485.0	160.0	61.34
	200	47	142	-490.2	110.0	73.42

Table 4.15 EDX data for mild steel after 3 hours immersion in 1M H_2SO_4 in the presence and absence of 200 ppm DPBD

S. No	Name of the sample	Element	Weight (%)	Atomic weight (%)
1.	BLANK	C	2.19	5.64
		O	28.38	54.92
		S	1.80	1.74
		Fe	66.78	37.02
2.	DPBD	C	17.12	25.53
		O	3.33	64.61
		N	1.79	2.29
		S	0.17	0.10
		Fe	23.14	7.39

Table 4.16 AFM data for mild steel surface after 3 hours of immersion in 1M H_2SO_4 in the absence and presence of 200 ppm DPBD

Specimen	Peak – valley height (nm)	Average roughness (nm) S_a	Root mean square (nm) S_q
Polished mild steel	1005.46	104.92	137.43
BLANK	1652.62	160.65	202.54
DPBD	1195.95	107.57	142.84

Figures
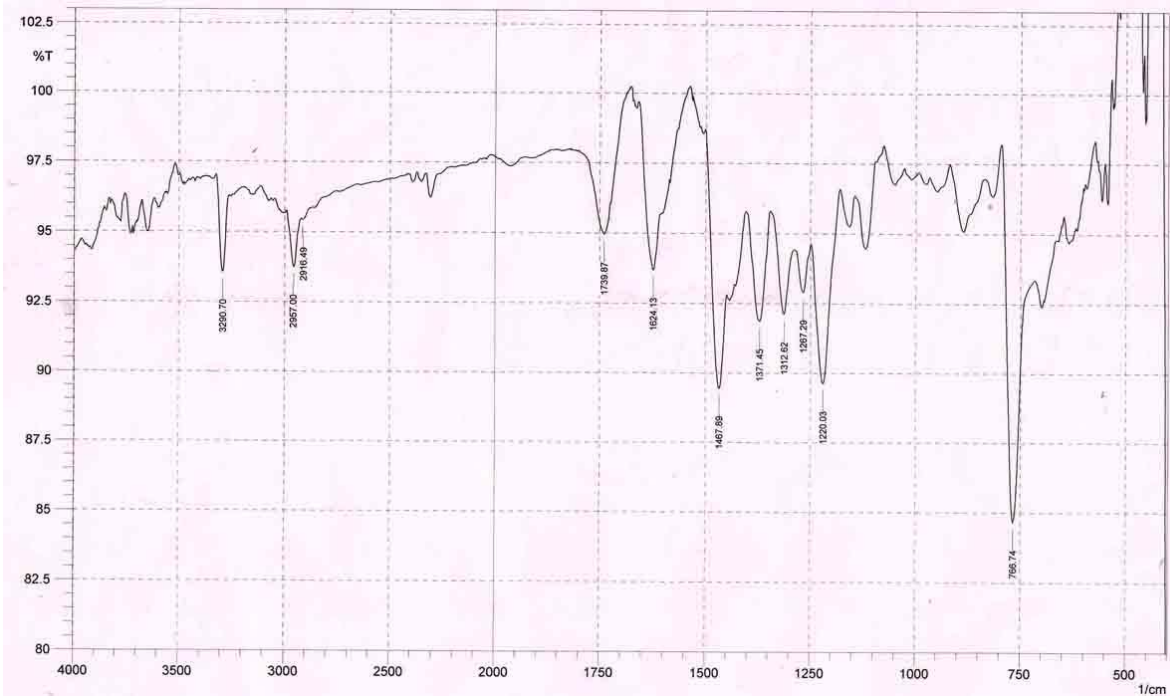
Figure 4.1 FTIR spectra of chalkone
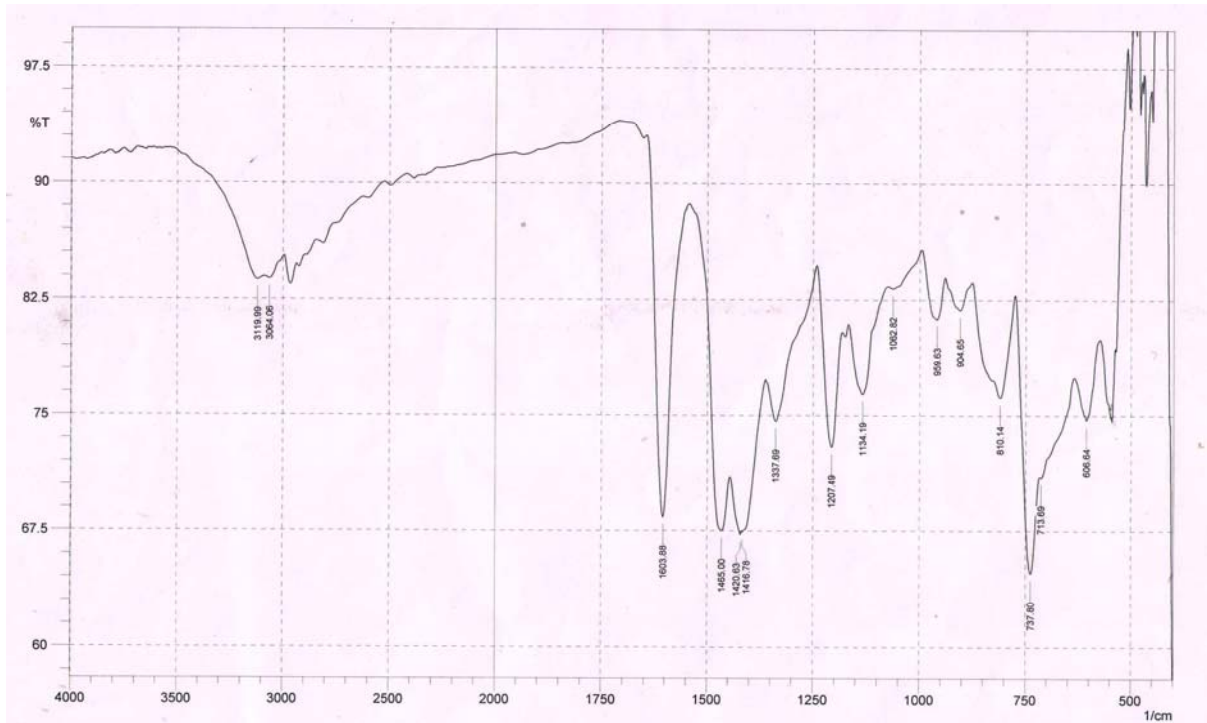
Figure 4.2 FTIR spectra of TEBD
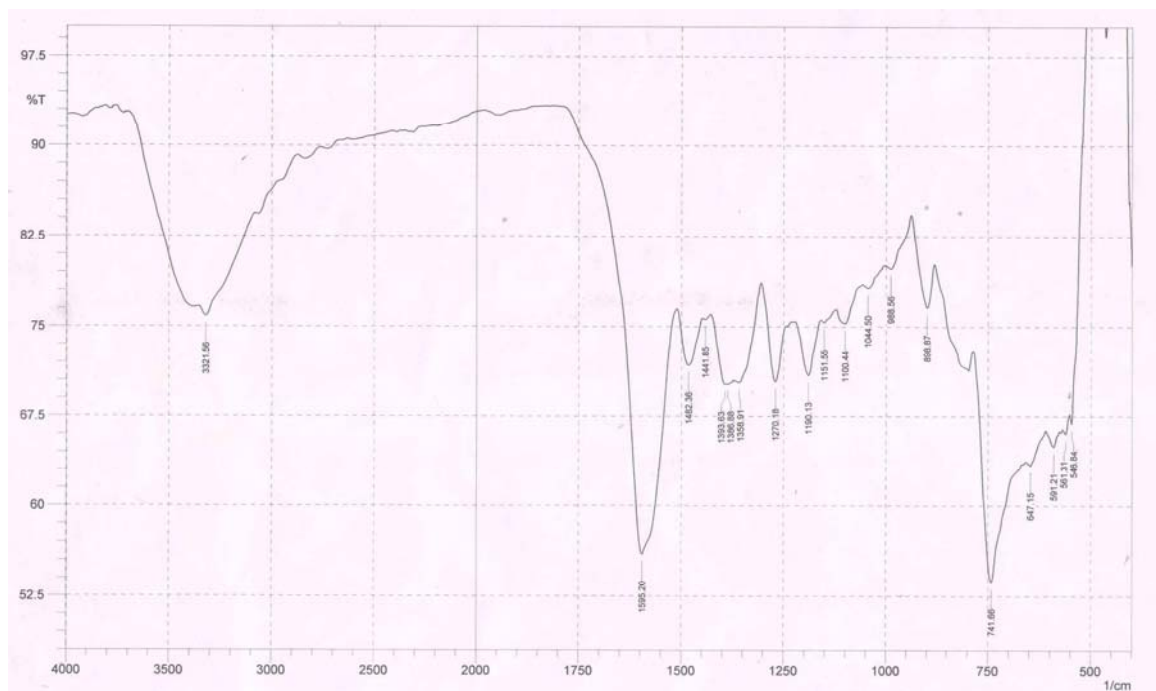
Figure 4.3 FTIR spectra of MBD
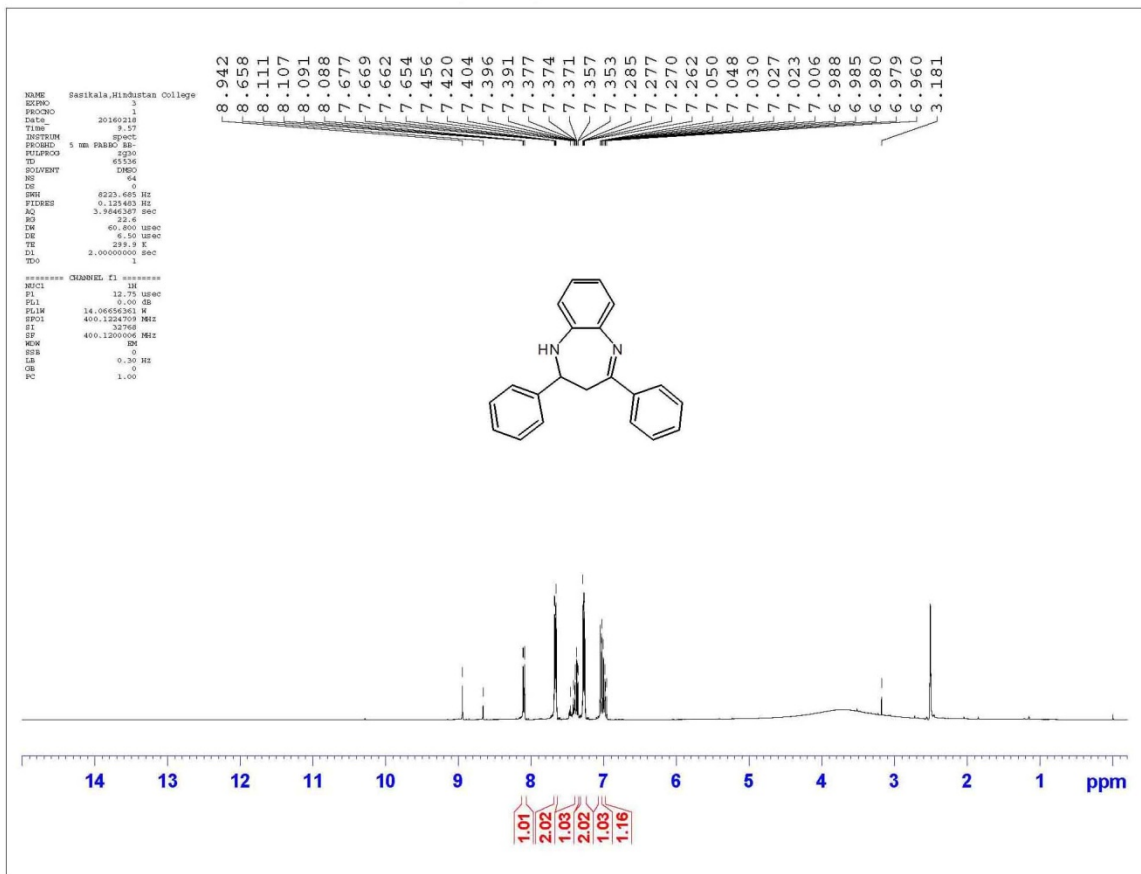
Figure 4.4 ^{1}H NMR spectra of DPBD
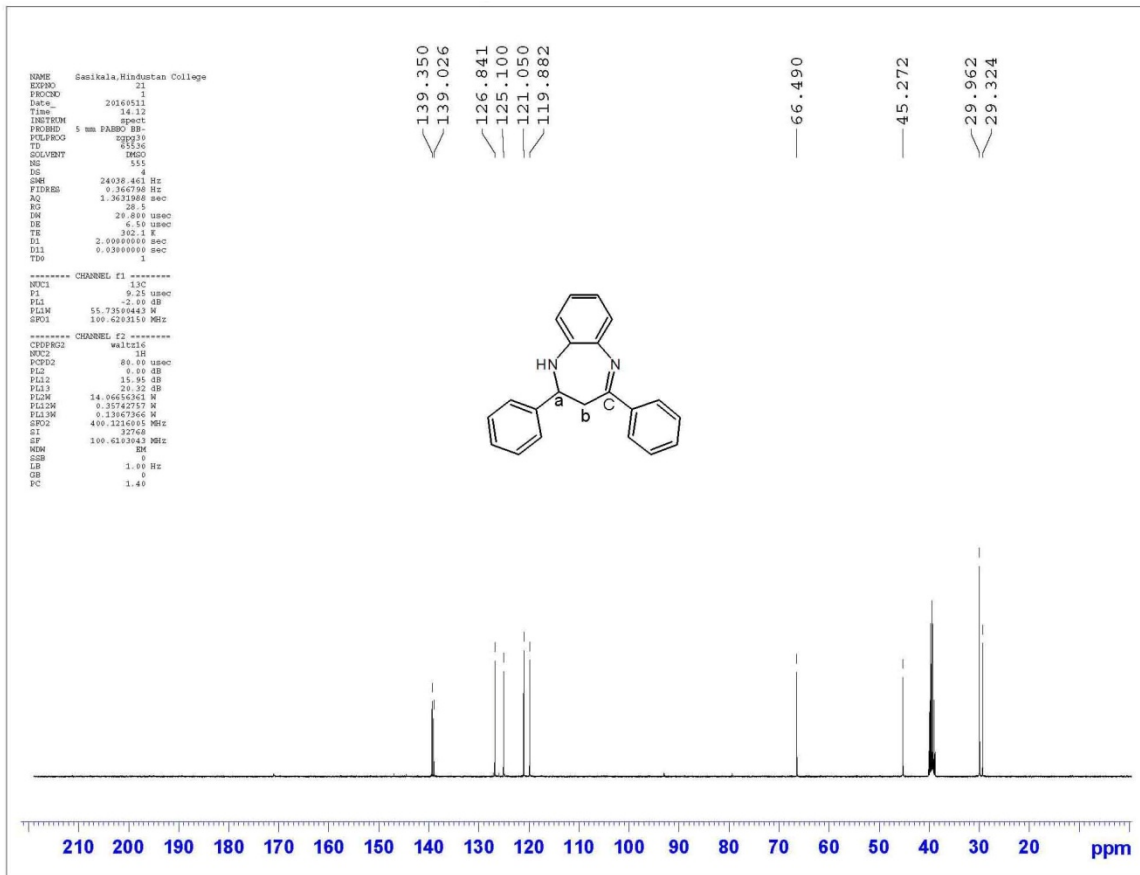
Figure 4.5 ^{13}C NMR spectra of DPBD
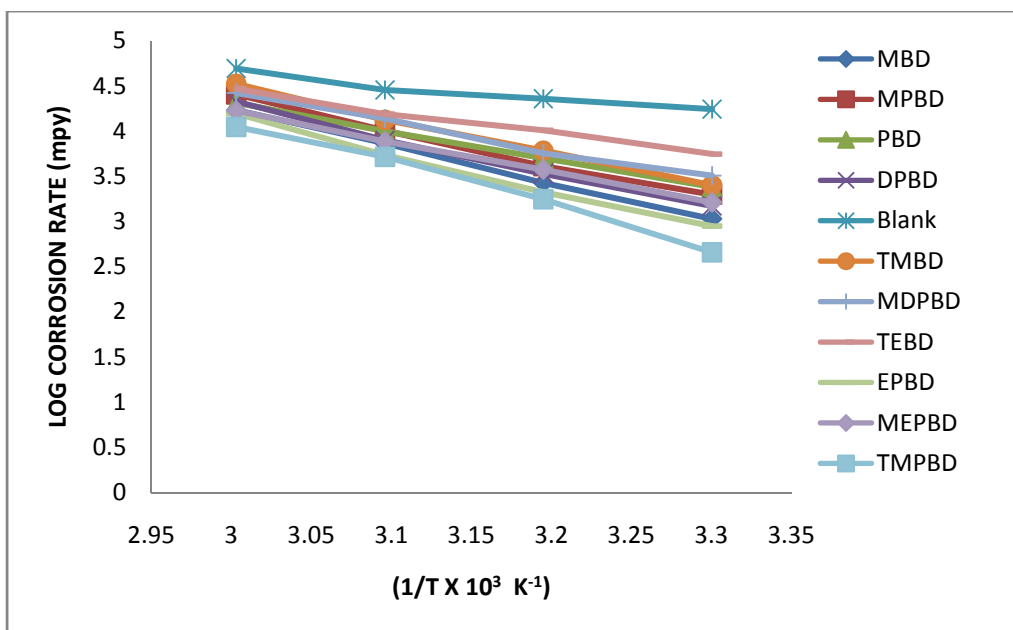
Figure 4.6 Arrhenius plots for corrosion of mild steel in 1M H_2SO_4 solution in the absence and presence of benzodiazepines
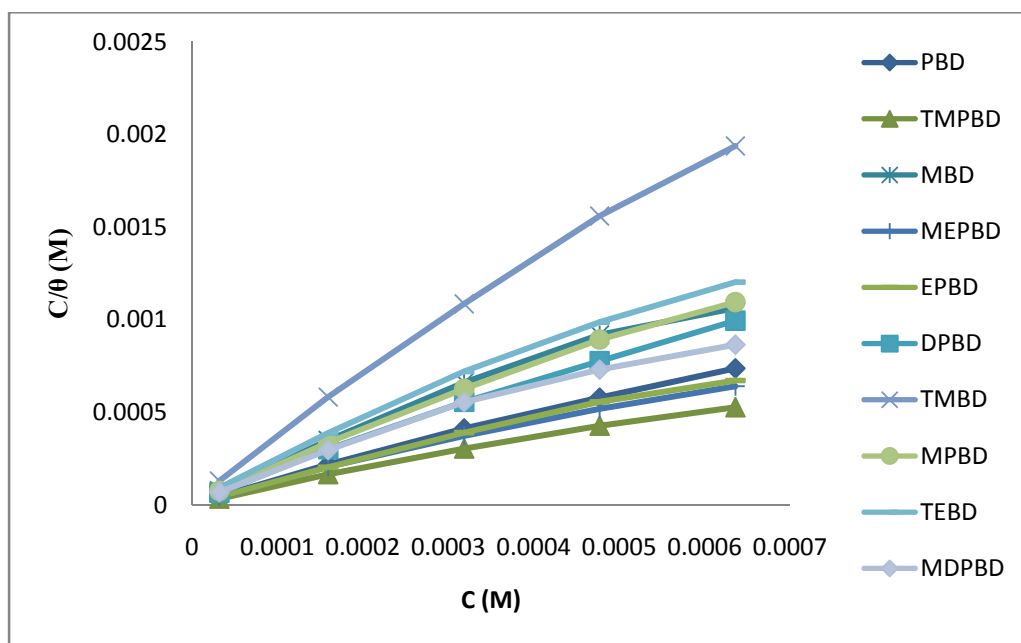
Figure 4.7 Langmuir plots for benzodiazepines in 1M H_2SO_4
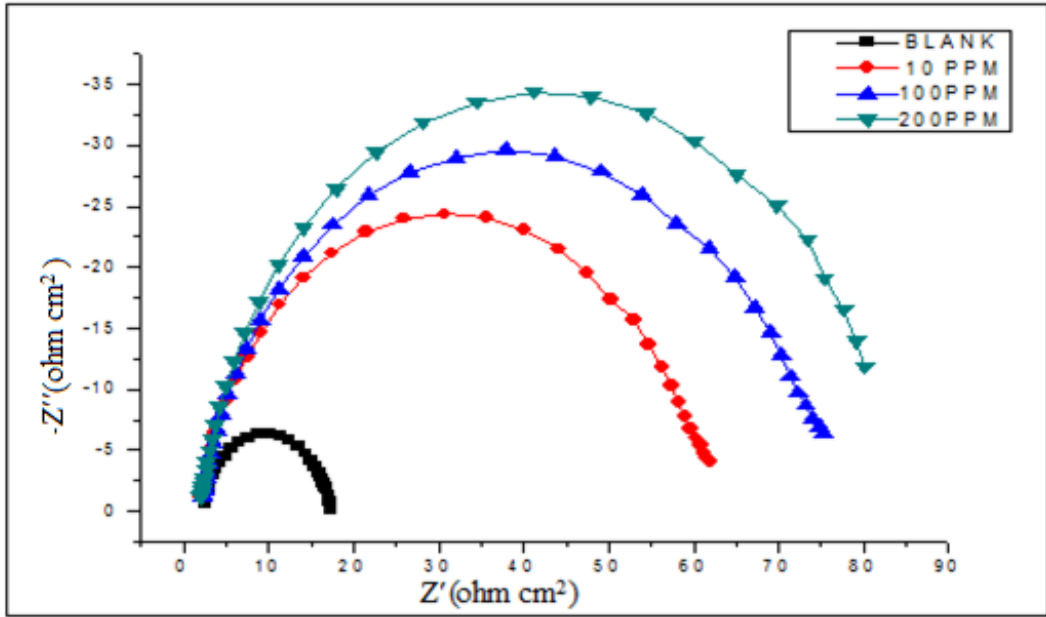
Figure 4.8 Nyquist diagram for mild steel in 1M H_2SO_4 for selected concentrations of benzodiazepine MDPBD
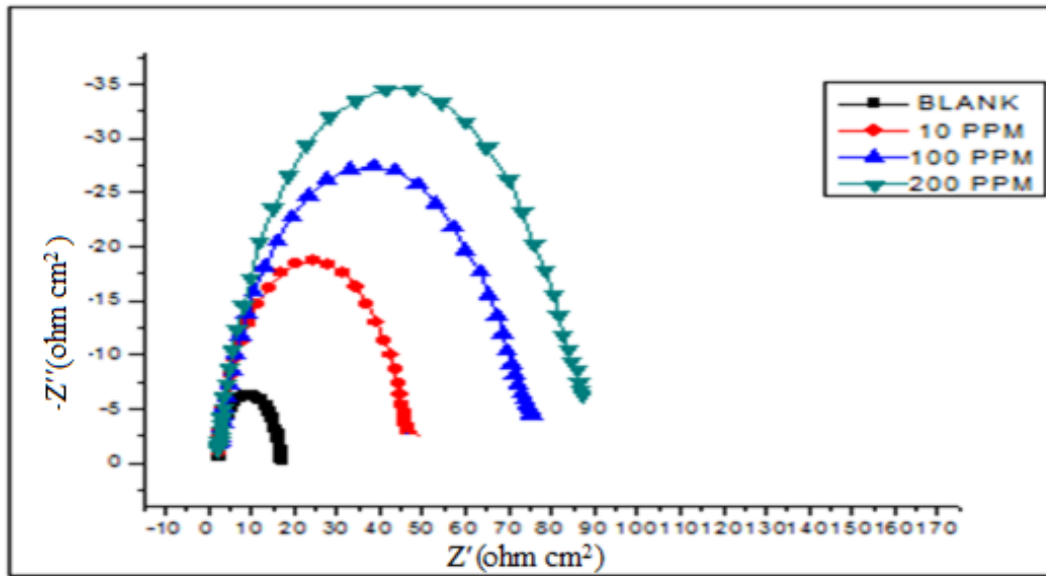
Figure 4.9 Nyquist diagram for mild steel in 1M H_2SO_4 for selected concentrations of benzodiazepine DPBD
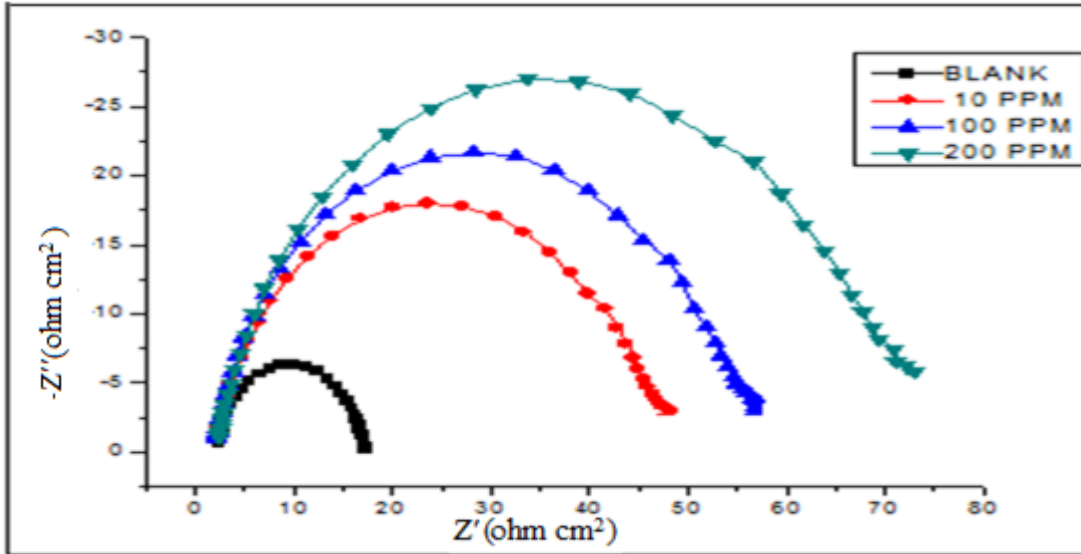
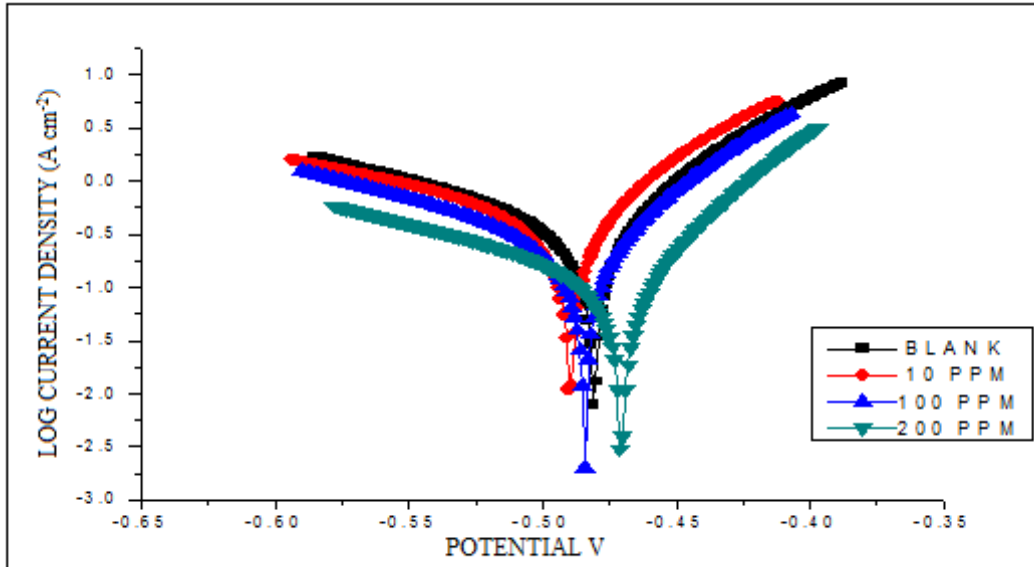**Figure 4.10** Nyquist diagram for mild steel in 1M H_2SO_4 for selected concentrations of benzodiazepine MPBD
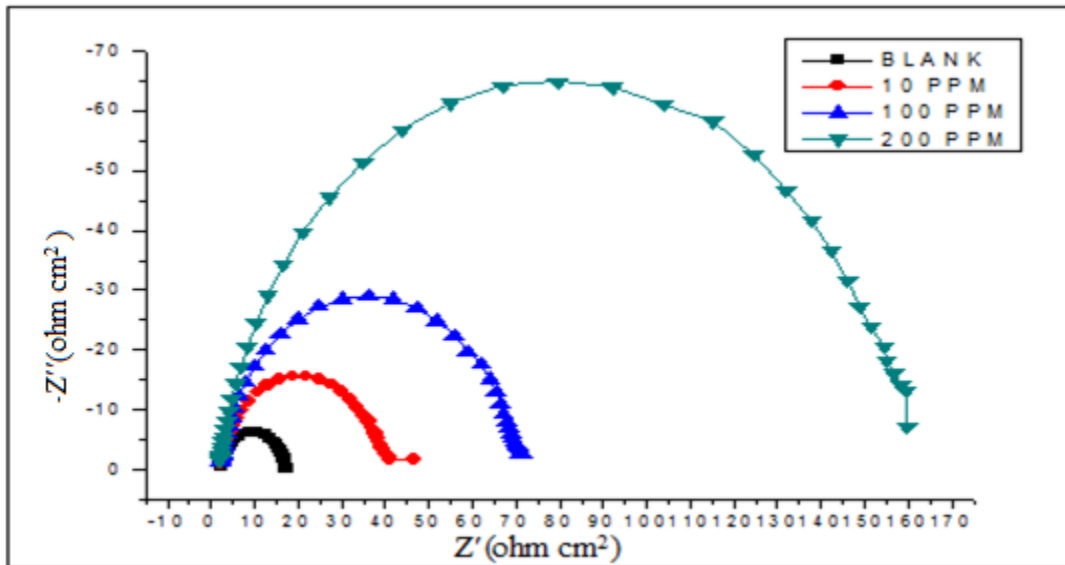
Figure 4.11 Nyquist diagram for mild steel in 1M H_2SO_4 for selected concentrations of benzodiazepine TEBD
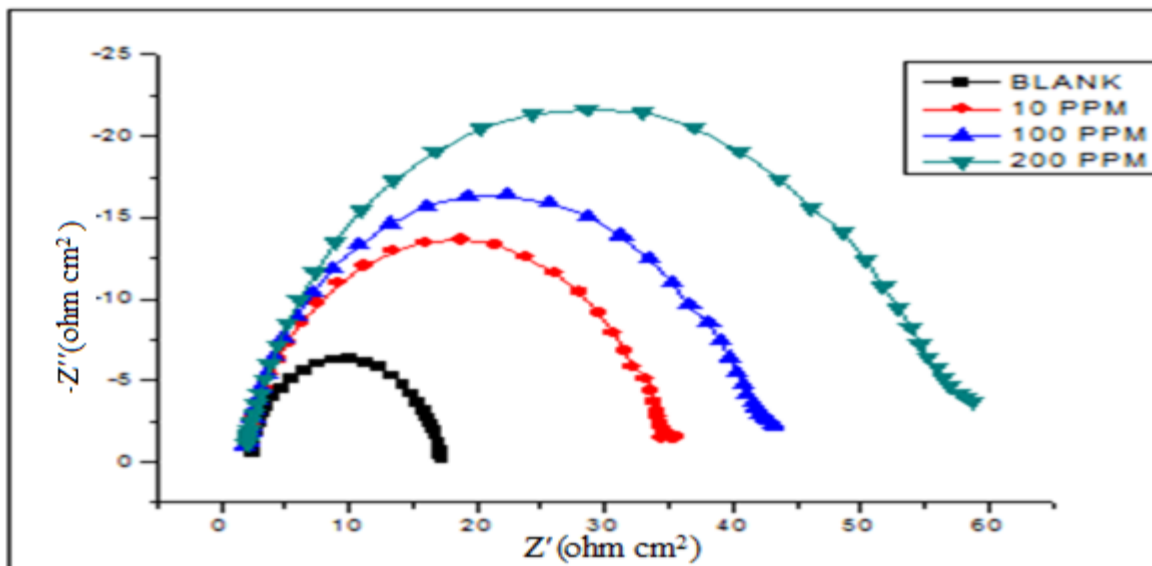
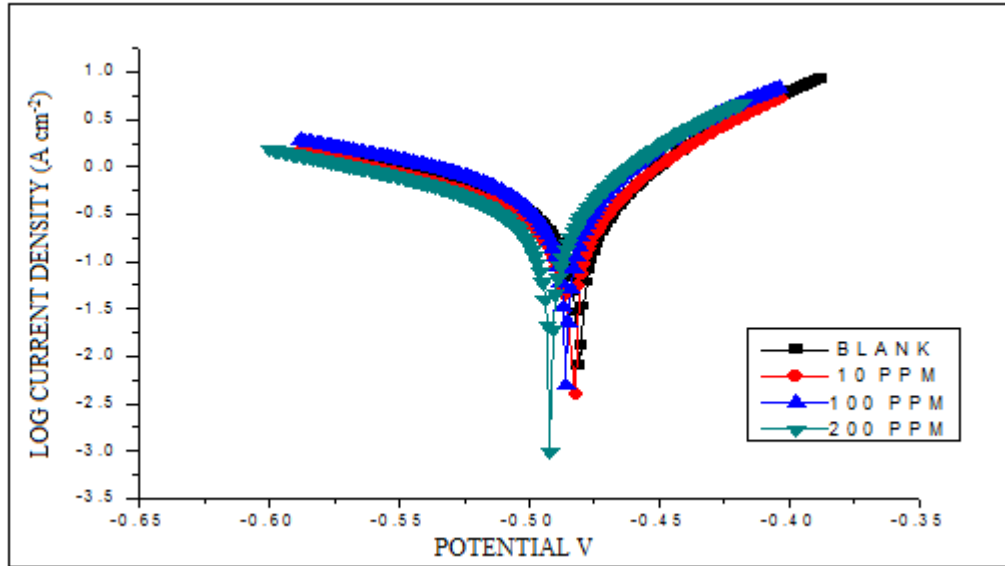**Figure 4.12** Nyquist diagram for mild steel in 1M H_2SO_4 for selected concentrations of benzodiazepine TMBD
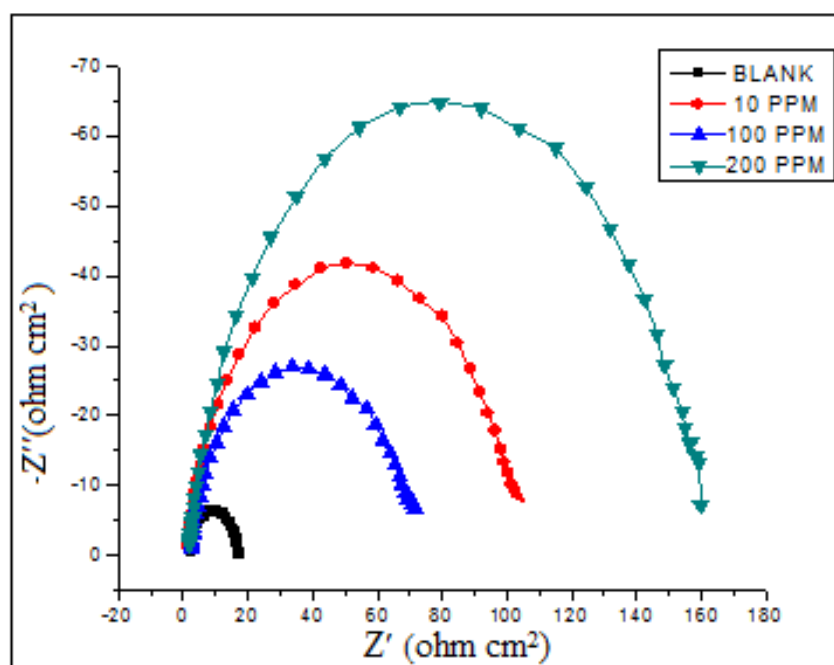
Figure 4.13 Nyquist diagram for mild steel in 1M H_2SO_4 for selected concentrations of benzodiazepine TMPBD
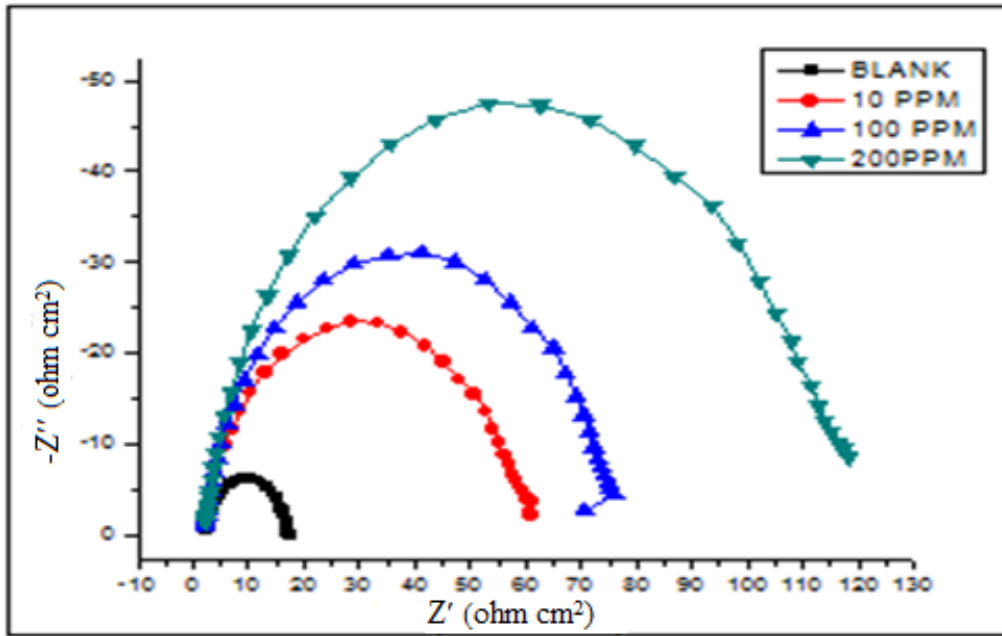
Figure 4.14 Nyquist diagram for mild steel in 1M H_2SO_4 for selected concentrations of benzodiazepine EPBD
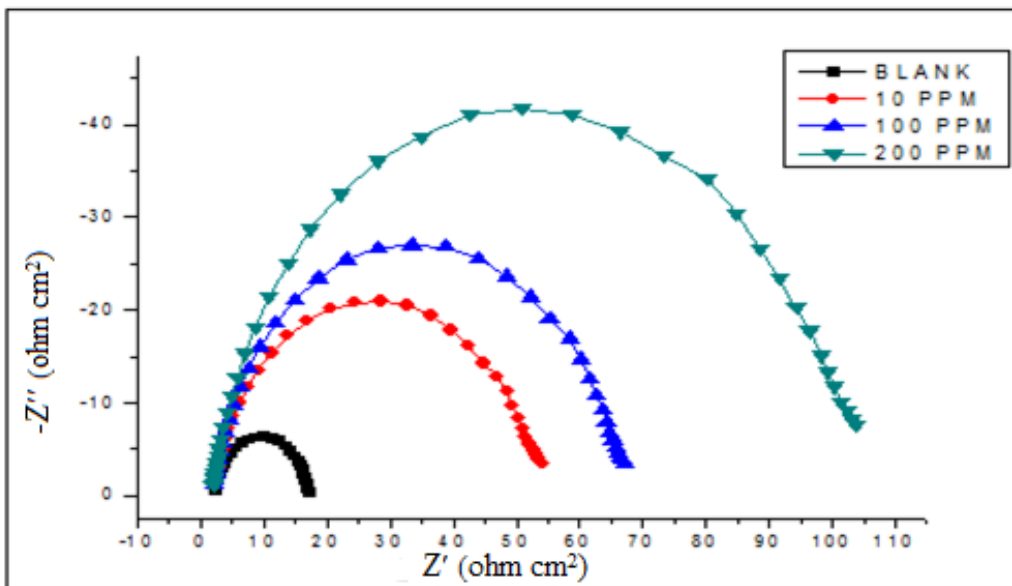

Figure 4.15 Nyquist diagram for mild steel in 1M H_2SO_4 for selected concentrations of benzodiazepine MEPBD
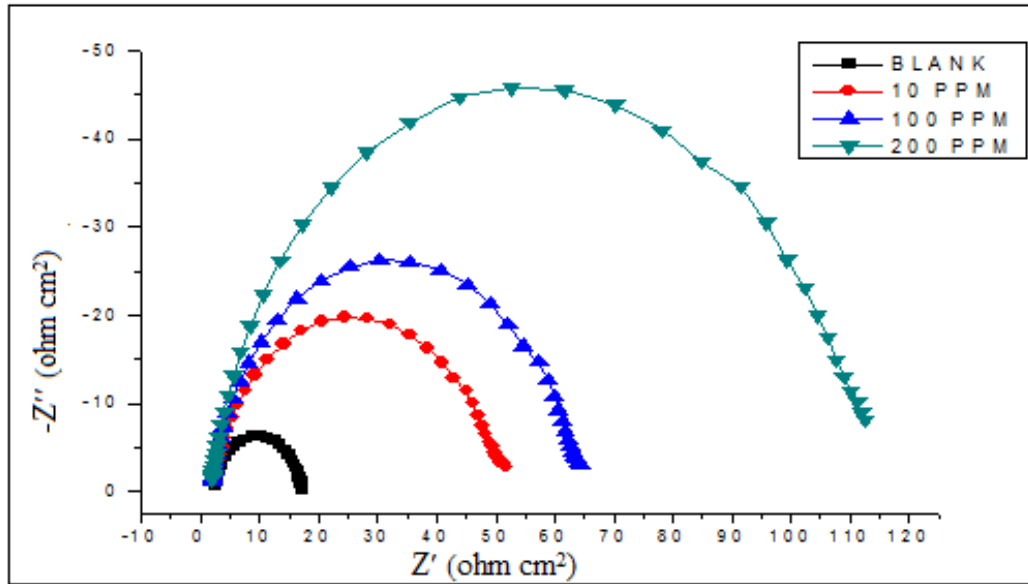
Figure 4.16 Nyquist diagram for mild steel in 1M H_2SO_4 for selected concentrations of benzodiazepine PBD
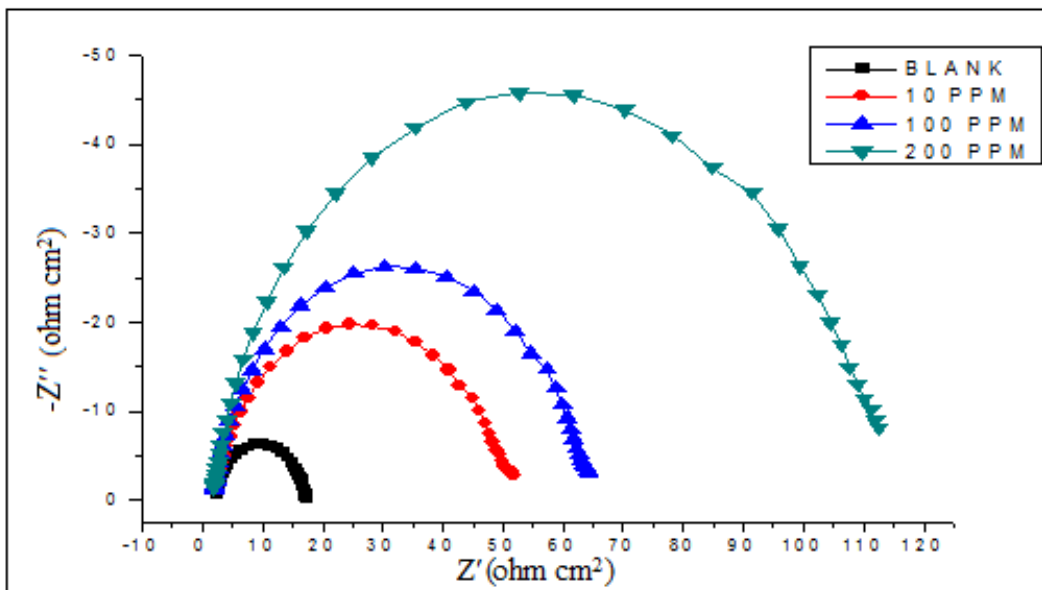
Figure 4.17 Nyquist diagram for mild steel in 1M H_2SO_4 for selected concentrations of benzodiazepine MBD
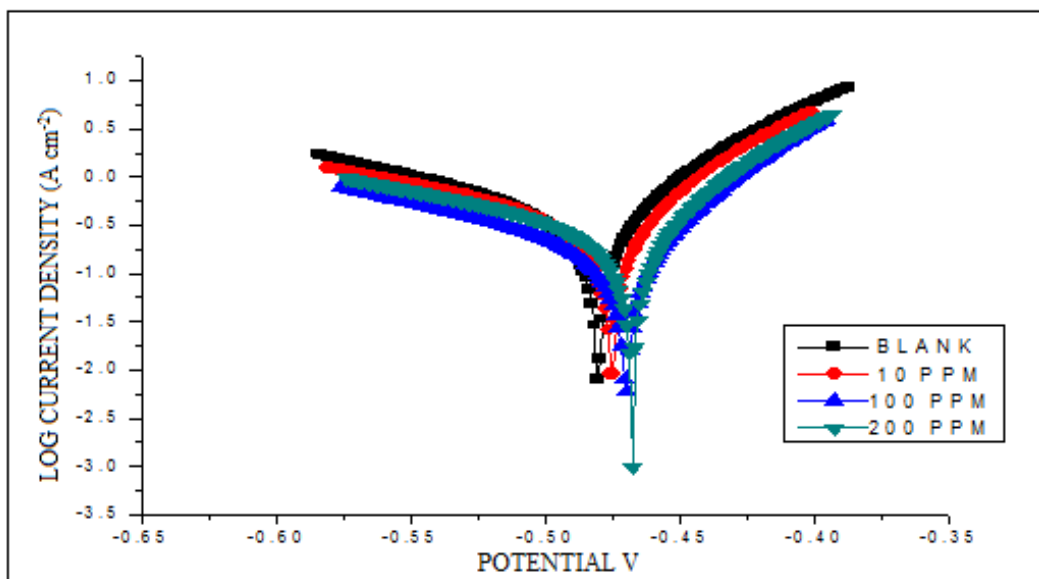
Figure 4.18 Polarization curves for mild steel in 1M H_2SO_4 for selected concentrations of benzodiazepine MDPBD
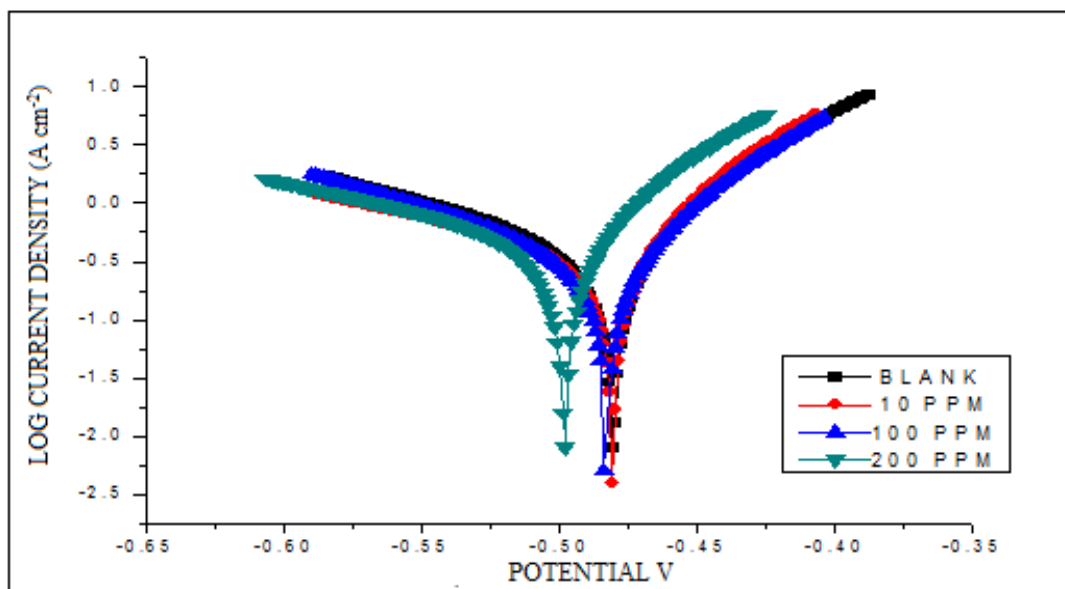

Figure 4.19 Polarization curves for mild steel in 1M H_2SO_4 for selected concentrations of benzodiazepine DPBD
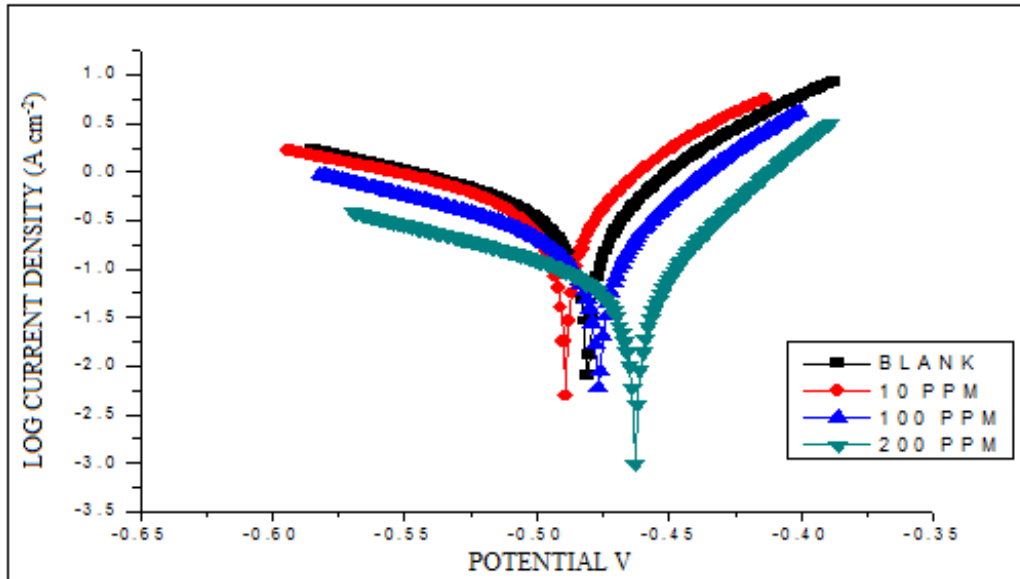
Figure 4.20 Polarization curves for mild steel in 1M H_2SO_4 for selected concentrations of benzodiazepine MPBD
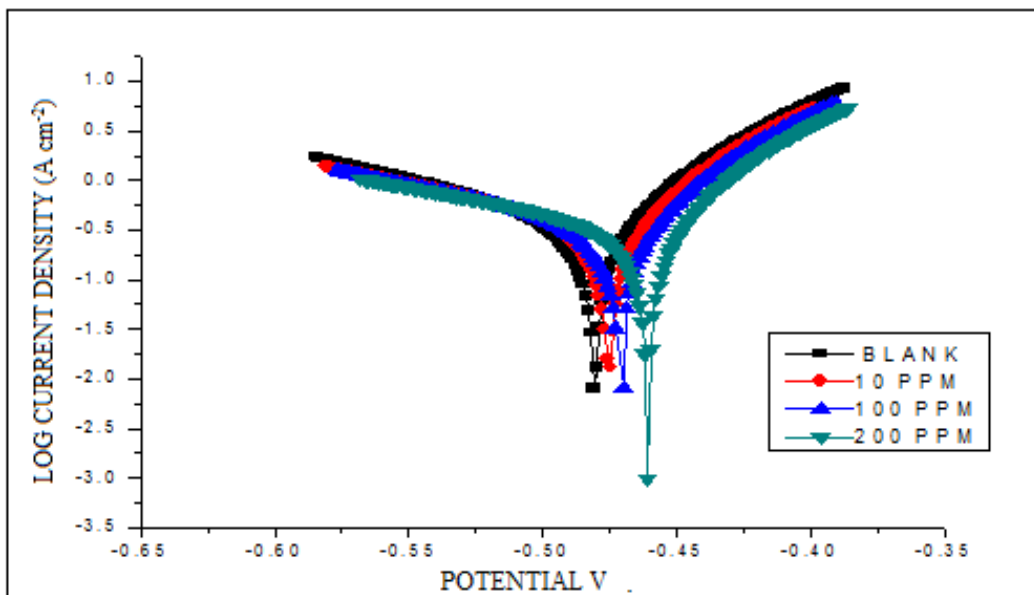

Figure 4.21 Polarization curves for mild steel in 1M H_2SO_4 for selected concentrations of benzodiazepine TEBD
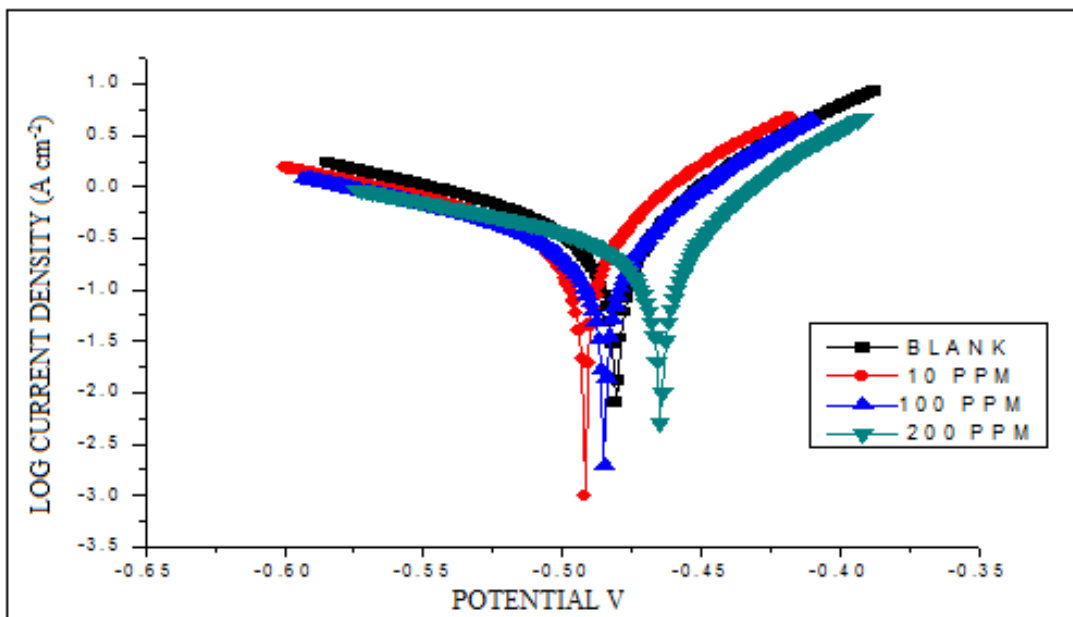
Figure 4.22 Polarization curves for mild steel in 1M H_2SO_4 for selected concentrations of benzodiazepine TMBD
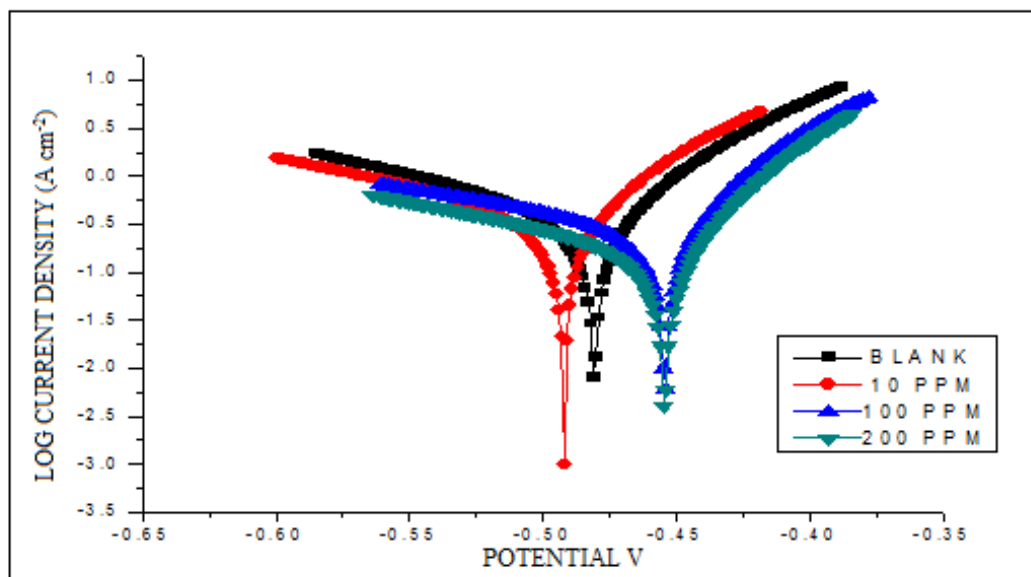

Figure 4.23 Polarization curves for mild steel in 1M H_2SO_4 for selected concentrations of benzodiazepine TMPBD
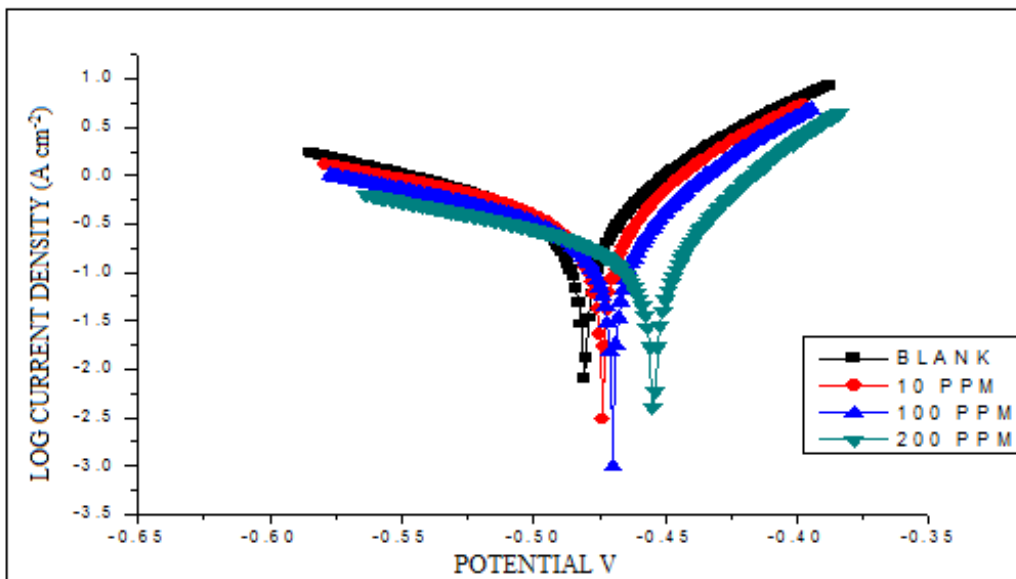
Figure 4.24 Polarization curves for mild steel in 1M H_2SO_4 for selected concentrations of benzodiazepine EPBD
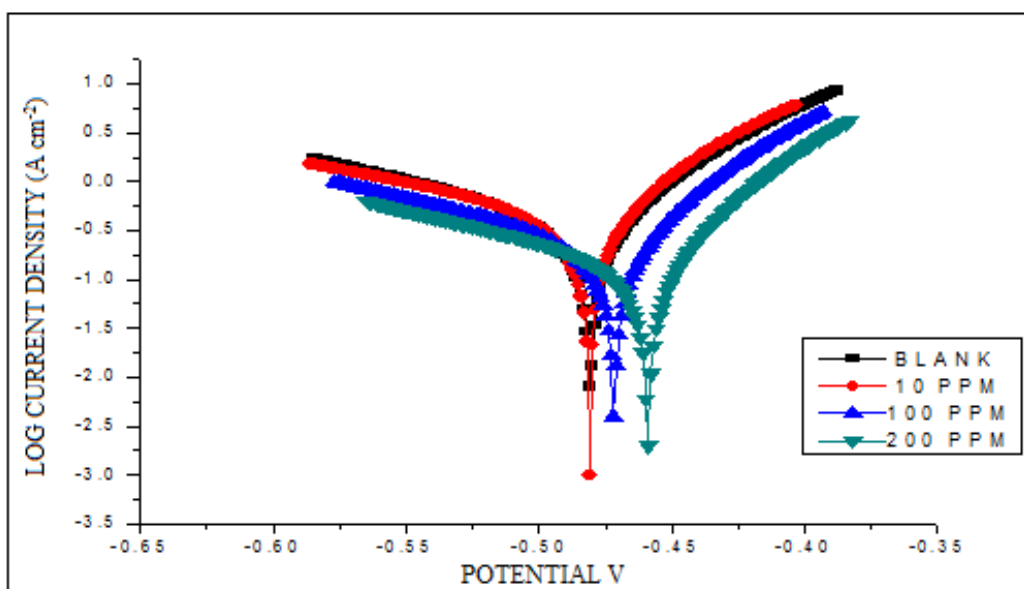
Figure 4.25 Polarization curves for mild steel in 1M H_2SO_4 for selected concentrations of benzodiazepine MEPBD

Figure 4.26 Polarization curves for mild steel in 1M H_2SO_4 for selected concentrations of benzodiazepine PBD

Figure 4.27 Polarization curves for mild steel in 1M H_2SO_4 for selected concentrations of benzodiazepine MBD
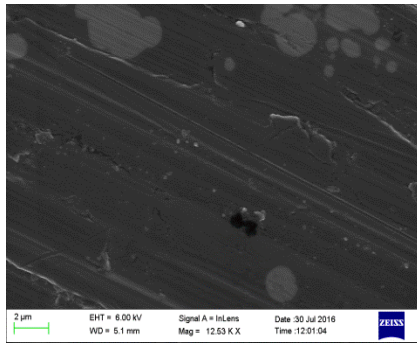
(a)
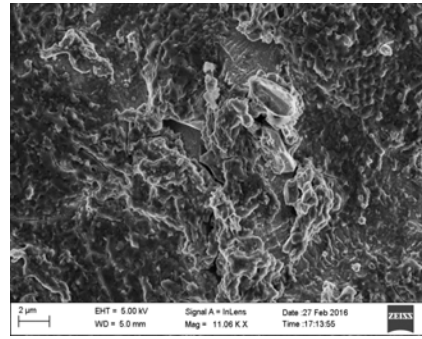
(b)
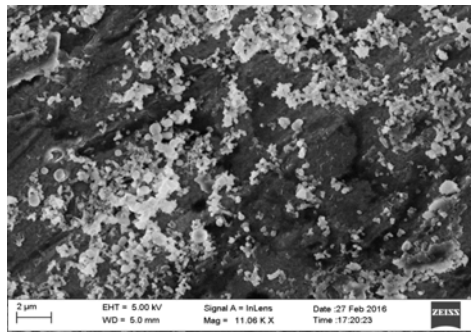
(c)

Figure 4.28 Scanning electron micrograph of mild steel specimen (a) Polished (b) After immersion in 1M H_2SO_4 (c) After immersion in 1M H_2SO_4 containing DPBD
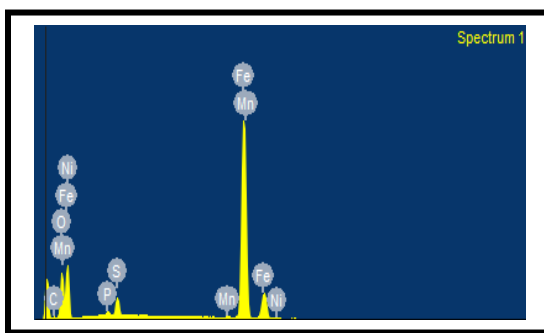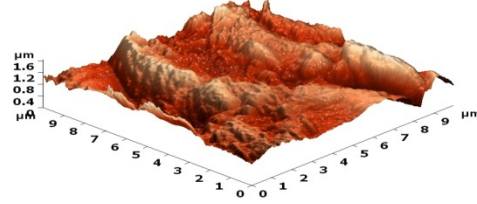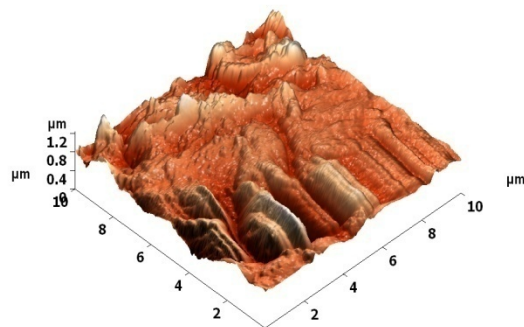

(a)
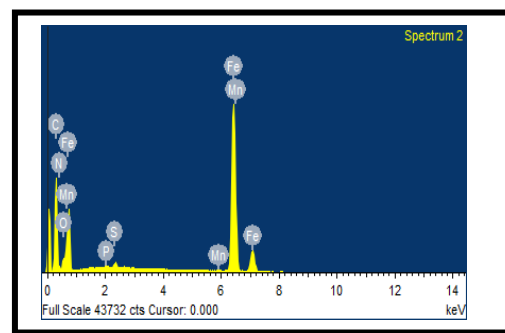
(b)

Figure 4.29 EDX spectra of mild steel immersed in 1M H_2SO_4 containing (a) 1M H_2SO_4 (b) DPBD
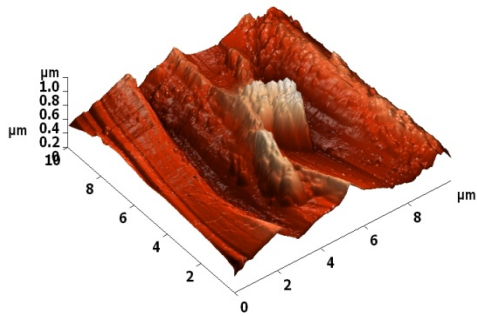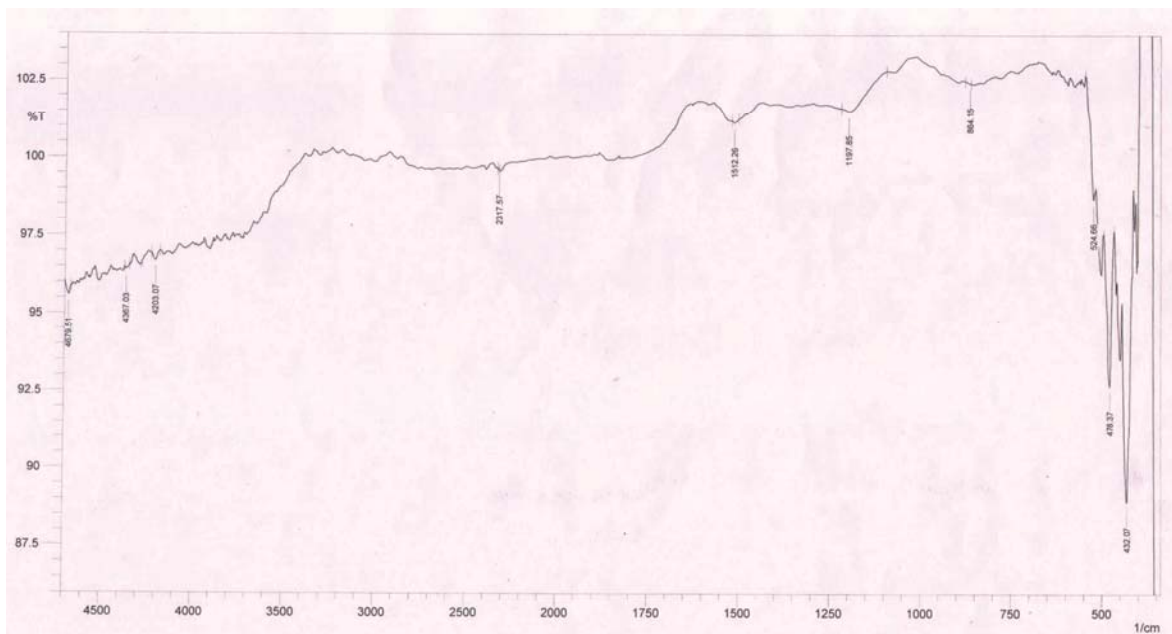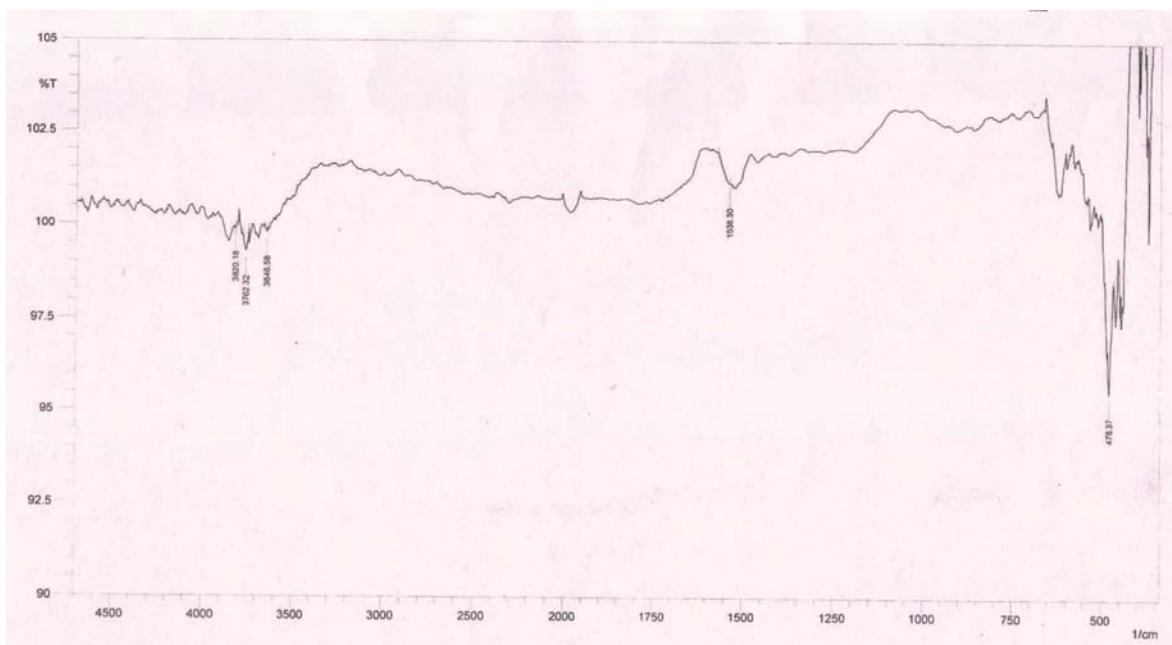
(a)

(b)

(c)

Figure 4.30 3D AFM topography of (a) bare mild steel (b) mild steel immersed in
1M H_2SO_4 (c) Mild steel immersed in 1M H_2SO_4 containing DPBD

Figure 4.31 FTIR spectra of mild steel immersed in 1M H_2SO_4

Figure 4.32 FTIR spectra of mild steel after immersion in 1M H_2SO_4 containing 200 ppm of DPBD